PROCEEDINGS A

royalsocietypublishing.org/journal/rspa

Research





Cite this article: Pourahmadian F, Haddar H. 2023 Ultrasonic imaging in highly heterogeneous backgrounds. *Proc. R. Soc. A* **479**: 20220721.

https://doi.org/10.1098/rspa.2022.0721

Received: 30 October 2022 Accepted: 27 January 2023

Subject Areas:

applied mathematics, acoustics, wave motion

Keywords:

differential evolution indicators, imaging in unknown backgrounds, randomly heterogeneous solids, geometric evolution, elastic transformation, inverse scattering

Author for correspondence:

F. Pourahmadian e-mail: fapo3151@colorado.edu

Ultrasonic imaging in highly heterogeneous backgrounds

F. Pourahmadian^{1,2} and H. Haddar^{3,4}

¹Department of Civil, Environmental and Architectural Engineering, and ²Department of Applied Mathematics, University of Colorado Boulder, Boulder, CO, USA

³INRIA Saclay Ile de France, 91120 Palaiseau, Paris, France ⁴UMA, ENSTA, Paris Tech, 828, Bd des Marechaux, Paris, France

FP, 0000-0003-2004-1427

This work formally investigates the differential evolution indicators as a tool for ultrasonic tracking of elastic transformation and fracturing in randomly heterogeneous solids. Within the framework of periodic sensing, it is assumed that the background at time t_{\circ} contains (i) a multiply connected set of viscoelastic, anisotropic and piecewise homogeneous inclusions, and (ii) a union of possibly disjoint fractures and pores. The support, material properties and interfacial condition of scatterers in (i) and (ii) are unknown, while elastic constants of the matrix provided. The domain undergoes progressive variations of arbitrary chemo-mechanical origins such that its geometric configuration and elastic properties at future times are distinct. At every sensing step t_{\circ}, t_{1}, \ldots , multi-modal incidents are generated by a set of boundary excitations, and the resulting scattered fields are captured over the observation surface. The test data are then used to construct a sequence of wavefront densities by solving the spectral scattering equation. The incident fields affiliated with distinct pairs of obtained wavefronts are analysed over the stationary and evolving scatterers for a suit of geometric and elastic evolution scenarios entailing both interfacial and volumetric transformations. The main theorem establishes the invariance of pertinent incident fields at the loci of static fractures and inclusions between a given pair of time steps, while certifying variation of the same fields over the modified regions. These results furnish a basis

© 2023 The Authors. Published by the Royal Society under the terms of the Creative Commons Attribution License http://creativecommons.org/licenses/by/4.0/, which permits unrestricted use, provided the original author and source are credited.

for theoretical justification of differential evolution indicators for imaging in complex composites which, in turn, enable the exclusive tomography of evolution in a background endowed with many unknown features.

1. Introduction

Many critical components in aerospace structures and energy systems are comprised of highly heterogeneous composites [1,2]. Examples include (a) single- and polycrystalline superalloys deployed in aeroengine and gas turbine blades [3], (b) interpenetrating phase metamaterials such as SiC-SiC composites used in accident-tolerant nuclear fuel claddings [4,5] and (c) multifunctional polymer matrix composites with a wide spectrum of applications thanks to their exceptional mechanical properties [6,7]. The topology and characteristics of such materials at micro- and meso-scales are often unknown, or only known to a limited extent because of variabilities in the manufacturing process [8,9] and/or ageing [10]. In addition, mechanisms of deterioration via corrosion, fatigue, irradiation and thermal cycling are yet to be fully understood. These processes, however, are responsible for continuous microstructural evolution leading to inevitable development of micro/macro cracks and volumetric damage zones which may result in the loss of functional performance in key components [11,12] (table 1).

Recent developments in sensing technology have resulted in a suite of imaging solutions germane to complex environments [13–20]. State-of-the-art examples include: penetrating-radar techniques [13], infrared thermography [14], laser shearography [15], X-ray computed tomography [16], acoustic tomography [17], ultrasonic surface wave methods [18], nonlinear ultrasound [19] and laser ultrasonic imaging [20]. Among which, ultrasonic sensing often emerges as the preferred (or the only feasible) imaging modality in many applications. Laser ultrasonics [21–23], in particular, has come under the spotlight for enabling non-contact actuation and measurement that is crucial for high-fidelity *in situ* monitoring of fabrication processes and advanced manufacturing [20,24,25].

Existing approaches to ultrasonic waveform inversion mostly rely on (a) distinct patterns in the measured scattered field associated with certain modes of propagation, (b) specific sensing configurations and (c) major postulates on the nature of wave motion in the background which, by and large, forgo the uncertain (yet important) scattering signatures affiliated with the specimen's microstructure. Such attributes expedite the data processing, yet entail the following impediments: (i) unstable reconstructions featuring many artefacts, (ii) significant errors in heterogeneous and anisotropic backgrounds where multiple scattering generates remarkable wave dispersion and attenuation, (iii) major restrictions on the geometry of incident and/or measurement grids, (iv) limited scalability beyond the controlled laboratory environment. Thus, there is a critical need for next-generation imaging solutions that carefully integrate state-of-theart instrumentation and advanced data analytic solutions to enable fast (yet robust) ultrasonic tomography of complex processes in uncertain or unknown environments.

Ongoing efforts in this vein are mainly focused on (a) optimization-based full-waveform inversion and (b) machine learning (ML). Inverse algorithms in (a) have so far been associated with tardy reconstructions due to their high computational cost. Lately, a few studies showed that the latter may be addressed by leveraging deep learning solutions pertinent to partial differential equations such as physics-informed neural networks [26,27]. However, the majority of paradigms in (b) make use of ML principles within the framework of existing logics for ultrasonic imaging so that the above-mentioned barriers are not fundamentally resolved. Nonetheless, ML schemes are shown to facilitate the implementation of various imaging solutions, and may serve as effective post-processing tools for image enhancement [28–30].

In applied mathematics, in parallel, over two decades of research in inverse scattering and transmission eigenvalues has given rise to a suite of rigorous algorithms for non-iterative waveform inversion [31–35]. Recently, sampling-based approaches to inverse scattering have

been applied to laser-ultrasonic test data [36]. The results demonstrate superior reconstructions in terms of quality and resolution compared to conventional methods. In addition, introduction of the differential evolution indicators [37] as a tool for waveform tomography in unknown media showcases a unique opportunity to achieve the above-mentioned goal of real-time laser-based monitoring. The differential indicators have so far been theoretically established for (i) acoustic imaging of obstacles in periodic and random media [38,39], and (ii) elastic-wave imaging of fractures in monolithic solids [40,41]. A rigorous justification of this imaging modality for its potentially dominant field of application i.e. ultrasonic tomography in complex composites—where the background features a random distribution of heterogeneities and discontinuities of unknown support and material characteristics which are subject to both interfacial and volumetric evolution—is still lacking. The present study is an effort towards establishing the differential evolution indicators in the general case of solids. In this vein, special attention is paid to pose the forward scattering problem in a broad sense by taking advantage of contributions on the nature of transmission eigenvalues in elastodynamics [42–48].

More specifically, the direct problem formulates sequential experiments conducted on a randomly structured composite such that at every sensing step t_{\circ}, t_{1}, \ldots , the specimen features an arbitrary networks of pores and fractures along with a set of viscoelastic, anisotropic and heterogeneous inclusions embedded in an elastic matrix. Properties of the binder are assumed to be known, while the support, material properties and interfacial condition of scatterers are a priori unknown and subject to spatio-temporal evolution. In this setting, boundary excitations at every time step give rise to distinct scattering footprints on the measurement surface. The idea is to use the sequence of scattered field measurements to design an imaging functional endowed with appropriate invariance with respect to stationary scatterers between any pairs of time steps such that the associated reconstructions uniquely expose the support of mechanical evolution in a given timeframe without the need to image the entire domain which may be insurmountable. To this end, the conditions for well-posedness of the forward problem are identified. The set of spectral scattering equations is then defined for waveform inversion. At every time step, the affiliated scattering operator and its related properties are carefully analysed in order to construct a sequence of approximate solutions to the scattering equation with strong convergence characteristics under a certain condition. The obtained solutions, i.e. wavefront densities, are then used to specify a set of incident fields over a generic model of the background, which forms the basis for differential imaging indicators. Next, the incidents corresponding to distinct pairs of wavefronts are analysed over the stationary and evolving scatterers for a suite of geometric and elastic evolution configurations. In the general case of solids, the latter involves a number of novel scenarios including (a) fracturing at bimaterial interfaces, (b) elastic transformation and/or expansion of fractured inclusions and (c) elastic conversion of microcracked damage zones. The main theorem establishes the invariance of incident fields at the loci of stationary fractures and inclusions, while certifying variation of the same fields over the evolved regions. These results pave the way for differential tomography of evolution in unknown backgrounds.

In the sequel, table 1 provides the list of main symbols, §2 provides the geometric and mechanistic description of the direct scattering problem and §§3 and 4 specify the fundamental properties of scattering operators. The main theorems in §5 establish the behaviour of differential indicators in the case of composites. Section 6 is dedicated to a numerical implementation and discussion of the results.

2. Preliminaries

Consider periodic illumination of mechanical evolution in a randomly structured composite shown in figure 1. At the first sensing step $t=t_\circ$, the specimen $\mathcal{B}\subset\mathbb{R}^3$ is comprised of (i) a linear, elastic, isotropic and homogeneous binder of mass density $\rho\in\mathbb{R}$ and Lamé parameters $\mu,\lambda\in\mathbb{R}$, (ii) a union of bounded inclusions $\mathcal{D}_\circ^\star\cup\mathcal{D}_\circ^\varrho=\mathcal{D}_\circ\subset\mathcal{B}$ with Lipschitz boundaries composed of penetrable \mathcal{D}_\circ^\star and impenetrable $\mathcal{D}_\circ^\varrho$ components where in the former case, the inclusions may

Table 1. Nomenclature

$t \in \{t_{\circ}, t_{1}, t_{2}, \ldots\}$	time sequence of sensing
ξ	position vector
I _m	mth-order symmetric identity tensor
R, 3	real and imaginary parts of a complex-valued quantity
n	unit outward normal to a boundary
ℓ_{\circ}	reference length scale
\mathcal{B}	specimen
$\partial \mathcal{B}_t$	Neumann part of the specimen's external boundary
\mathcal{B}_{κ}^{-}	binder support at t_{κ} , $\kappa = 0, 1, 2, \dots$
$ ho, \mu, \lambda$	binder's mass density and Lamé parameters
\mathcal{D}_{κ}	volumetric scatterers at t_{κ} , $\kappa=\circ$, 1, 2,
$\mathcal{D}_{\kappa}^{\star}$, \mathcal{D}_{κ}^{o}	penetrable and impenetrable inclusions at t_{κ} , $\kappa=\circ$, 1, 2, \ldots
ρ_{κ} , C_{κ}	mass density and viscoelasticity tensor characterizing $\mathcal{D}_{\kappa}^{\star}$
Γ_{κ}	fractures at t_{κ} , $\kappa = 0, 1, 2, \dots$
K_{κ}	interfacial stiffness matrix on $arGamma_{\kappa}$
Γ_{κ}^{o}	traction-free cracks at t_{κ} , $\kappa=\circ$, 1, 2, \ldots
ω	illumination frequency
λ_{s}	shear wavelength in the binder
τ	external traction, wavefront density
$u^{\rm f}$, $t^{\rm f}$	free-field displacement and traction
u^{κ} , w^{κ}	total field in the binder and inclusions at t_{κ} , $\kappa=\circ$, 1, 2, \ldots
G, Σ	Green's displacement and stress tensors
$oldsymbol{v}^{\kappa}$	scattered field at t_κ , $\kappa=\circ$, 1, 2, \ldots
$t[\cdot]$	traction vector associated with a displacement field
[.]	jump in a vector field across a discontinuity surface
$\check{\mathcal{D}}_{i-1}^{\star},\check{\mathcal{D}}_{i-1}^{o}$	time-invariant inclusions and pores between $[t_{i-1}, t_i], i \in \mathbb{N}$
$ ilde{\mathcal{D}}_{i-1}^{\star}, ilde{\mathcal{D}}_{i-1}^{o}$	modified inclusions and pores $[t_{i-1},\ t_i], i\in\mathbb{N}$
\mathcal{E}_i^\star	volumetric elastic transformation between $[t_{i-1},\ t_i], i\in\mathbb{N}$
\mathcal{E}_i^o	new pores/cavities formed between $[t_{i-1},\ t_i], i\in\mathbb{N}$
$\check{\Gamma}_{i-1}$	stationary fractures between $[t_{i-1},t_i],i\in\mathbb{N}$
$ ilde{\Gamma}_i$	elastically modified interfaces between $[t_{i-1},\ t_i], i\in\mathbb{N}$
$\hat{\Gamma}_i$	newborn discontinuities within $[t_{i-1}, t_i], i \in \mathbb{N}$
$arLambda_{\kappa}$	spectral scattering operator at t_{κ} , $\kappa=\circ$, 1, 2, \ldots
$\Lambda_{\kappa_{\sharp}}$	positive and self-adjoint scattering operator computed from A_{κ}
(.)*	adjoint operator
\mathcal{R}	range of an operator
L	trial dislocation

а	admissible displacement density on <i>L</i>
x_{\circ}	sampling point
R	unitary rotation matrix
Ψ^0	trial scattering pattern
$\mathfrak{J}^{\gamma}_{\kappa}$	regularized sequence of cost functions
γ	regularization parameter
\mathcal{G}_{κ}	constructed minimizer of $\mathfrak{J}^{\gamma}_{\kappa}$
$(u_{\kappa}^{\star}, w_{\kappa}^{\star})$	solution to the interior transmission problem at t_{κ} , $\kappa=\circ$, 1, 2,
Cinc Cops	incident and observation grids

scattered field captured at t_{κ} , $\kappa = \circ$, 1, 2, . . . , on the observation surface

differential evolution indicators associated with timespan $[t_{i-1}, t_i], i \in \mathbb{N}$

Table 1. (Continued.)

 $oldsymbol{v}_{\kappa}^{\mathsf{obs}}$

 $\mathfrak{D}_i, \mathfrak{D}_i$

be viscoelastic, anisotropic and multiply connected, and (iii) a network of discontinuity surfaces $\Gamma_{\circ} \subset \mathcal{B}$ characterized by the complex-valued and heterogeneous interfacial stiffness matrix $K_{\circ}(\xi)$ where $\xi \in \Gamma_{\circ}$ is the position vector. The specimen may be exposed to irradiation or chemical reactions as common producers of interfacial damage [49], and/or subject to thermal cycling, fatigue and shock-waves which are mostly responsible for volumetric degradation [50] so that at any future sensing steps $t = t_i > t_o$, $i \in \mathbb{N}$, the domain \mathcal{B} features an evolved set of inclusions $\mathcal{D}_i^{\star} \cup \mathcal{D}_i^o = \mathcal{D}_i \subset \mathcal{B}$ and interfaces $\Gamma_i \subset \mathcal{B}$ such that $\mathcal{D}_{i-1} \subset \mathcal{D}_i$ and $\Gamma_{i-1} \setminus \overline{\mathcal{D}_i^o} \subset \Gamma_i$, $\forall i \in \mathbb{N}$. For further clarity, let $\rho_{\kappa} = \rho_{\kappa}(\xi) > 0$ and $C_{\kappa} = C_{\kappa}(\xi)$, $\kappa = 0, 1, ...$, designate the mass density and (complexvalued) viscoelasticity tensor associated with the penetrable obstacles $\mathcal{D}_{\kappa}^{\star}$ at t_{κ} . Here, $(C_{\kappa}, \rho_{\kappa})$ are understood in a piecewise-constant sense i.e., $\mathcal{D}_{\kappa}^{\star}$ can be decomposed into N_{κ}^{\star} open, simply connected and non-overlapping subsets $\mathcal{D}_{\kappa}^{n} \subset \mathcal{D}_{\kappa}^{\star}$ (of Lipschitz boundaries) where both ρ_{κ} and C_{κ} are constants $\forall \xi \in \mathcal{D}_{\kappa}^{n}$, and $\overline{\mathcal{D}_{\kappa}^{\star}} = \bigcup_{n=1}^{N_{\kappa}^{\star}} \overline{\mathcal{D}_{\kappa}^{n}}$. It should be noted that $\forall t_{\kappa}, \mathcal{D}_{\kappa}^{\star}$ and \mathcal{D}_{κ}^{0} are assumed to be disjoint, i.e. $\overline{\mathcal{D}_{\kappa}^{*}} \cap \overline{\mathcal{D}_{\kappa}^{0}} = \emptyset$. In addition, the support of Γ_{κ} may be decomposed into N_{κ} smooth open subsets $\Gamma_n \subset \Gamma_{\kappa}$, $n=1,\ldots,N_{\kappa}$, such that $\Gamma_{\kappa} = \bigcup_{n=1}^{N_{\kappa}} \Gamma_n$. The support of Γ_n may be arbitrarily extended to a closed Lipschitz surface ∂D_n of a bounded simply connected domain D_n , so that the unit normal vector n to Γ_n coincides with the outward normal vector to ∂D_n . We assume that Γ_n is an open set (relative to ∂D_n) with a positive surface measure.

In this setting, let $\mathcal{E}_i^{\star} \cup \mathcal{E}_i^0$ and $\hat{\Gamma}_i \cup \tilde{\Gamma}_i$, respectively, specify the support of volumetric and interfacial evolution within $[t_{i-1}, t_i]$ for $i \in \mathbb{N}$ such that

$$\overline{\widehat{\Gamma}_{i}} := \overline{\Gamma_{i} \setminus \overline{\Gamma_{i-1}}}, \quad \overline{\widetilde{\Gamma}_{i}} := \overline{\left\{ \xi \in \Gamma_{i-1} \setminus \overline{\mathcal{D}_{i}^{0}} : K_{i-1}(\xi) \neq K_{i}(\xi) \right\}},
\overline{\mathcal{E}_{i}^{0}} := \overline{\mathcal{D}_{i}^{0} \setminus \overline{\mathcal{D}_{i-1}^{0}}}, \quad \overline{\mathcal{E}_{i}^{\star}} := \overline{\operatorname{supp}(C_{i} - C_{i-1}) \cup \operatorname{supp}(\rho_{i} - \rho_{i-1})}, \quad i \in \mathbb{N}.$$
(2.1)

At $t = t_{\circ}$, Specimen's external boundary $\partial \mathcal{B}$ and the binder's constants (λ, μ, ρ) are known which may be used to define a baseline model of the background. On the other hand, the support of pre-existing scatterers $\mathcal{D}_{\circ} \cup \Gamma_{\circ}$ and their designated properties $(\mathcal{C}_{\circ}, \rho_{\circ}, K_{\circ})(\xi)$ are unknown. Given sequential sensory data at t_{i-1} and t_i for $i \in \mathbb{N}$, the objective is to reconstruct the support of volumetric and interfacial evolution $\mathcal{E}_{i}^{\star} \cup \mathcal{E}_{i}^{o} \cup \hat{\Gamma}_{i} \cup \tilde{\Gamma}_{i}$ defined by (2.1).

Assumption 2.1. Let $\Gamma_{\kappa}^{o} \subset \Gamma_{\kappa}$ denote the union of traction-free cracks at t_{κ} such that

$$\overline{\Gamma_{\kappa}^{o}} := \overline{\left\{ \boldsymbol{\xi} \in \Gamma_{\kappa} : K_{\kappa}(\boldsymbol{\xi}) = 0 \right\}}, \quad \kappa = \circ, 1, \ldots,$$

then $\mathcal{B} \setminus \overline{\mathcal{D}_{\kappa}^{0} \cup \Gamma_{\kappa}^{0}}$ remains connected $\forall t_{\kappa}$.

Assumption 2.2. Let $\Re(\cdot)$ and $\Im(\cdot)$, respectively, denote the real and imaginary parts of a complex-valued quantity, and recall that the fourth-order tensor $C_{\kappa}(\xi)$ represents the viscoelastic

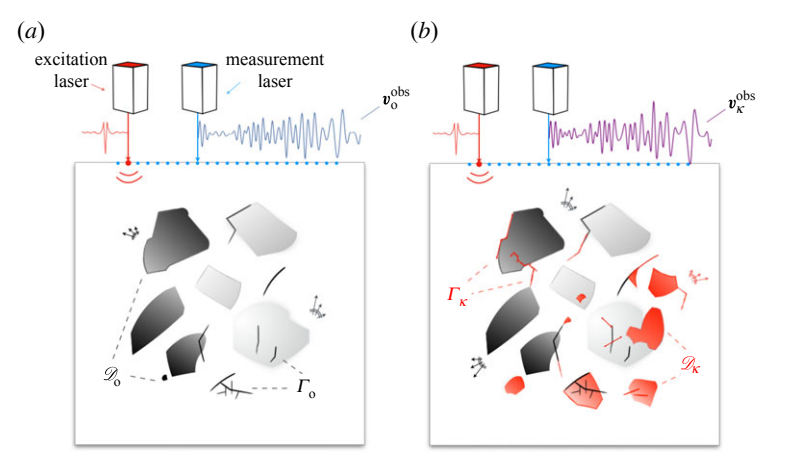


Figure 1. Ultrasonic sensing of evolution in a heterogeneous composite featuring a network of arbitrary inclusions, fractures and pores of unknown distribution, elastic properties and interfacial conditions: (a) primary experiments conducted at $t=t_{\circ}$ when a set of boundary excitations, interacting with the unknown pre-existing scatterers $\mathcal{D}_\circ \cup \Gamma_\circ$, induce the scattered field v_o^{obs} on the observation surface, and (b) secondary experiments performed sequentially at later times $t_i = \{t_1, t_2, \ldots\}$ when new and evolved scatterers $\mathcal{D}_{\kappa} \cup \Gamma_{\kappa}$ lead to distinct waveform measurements $\boldsymbol{v}_{\kappa}^{\text{ obs}}$.

and anisotropic behaviour of inclusions $\mathcal{D}_{\kappa}^{\star}$ at t_{κ} . Then, the real part of C_{κ} is bounded by piecewise-constant and strictly positive functions c_{κ} and c_{κ} , while the magnitude of its imaginary part is constrained by piecewise-constant and non-negative functions V_{κ} and V_{κ} such that $\forall \Phi \in$ $\mathbb{C}(\mathcal{D}_{\kappa}^{\star})^{3\times3}$,

$$\begin{cases} c_{\kappa} |\boldsymbol{\Phi}|^{2} \leq \Re(\boldsymbol{\Phi}: C_{\kappa}: \overline{\boldsymbol{\Phi}}) \leq c_{\kappa} |\boldsymbol{\Phi}|^{2} & \text{in } \mathcal{D}_{\kappa}^{\star} \\ v_{\kappa} |\boldsymbol{\Phi}|^{2} \leq -\Im(\boldsymbol{\Phi}: C_{\kappa}: \overline{\boldsymbol{\Phi}}) \leq v_{\kappa} |\boldsymbol{\Phi}|^{2} & \text{in } \mathcal{D}_{\kappa}^{\star} \end{cases}, \quad \kappa = 0, 1, \dots$$

$$(2.2)$$

Also, the interfacial stiffness matrix $K_{\kappa} \in L^{\infty}(\Gamma_{\kappa})^{3\times 3}$ is symmetric $\forall \kappa$, while satisfying $\overline{\varphi} \cdot \Im K_{\kappa}(\xi)$. $\varphi \leq 0, \forall \varphi \in \mathbb{C}(\Gamma_{\kappa})^3.$

Assumption 2.3. Let $C = \lambda I_2 \otimes I_2 + 2\mu I_4$ denote the binder's fourth-order elasticity tensor, wherein I_m (m = 2,4) designates the mth-order symmetric identity tensor. Then, given Poisson's ratio $\nu = \lambda/2(\lambda + \mu)$ and $\mathcal{B}_{\kappa}^{-} := \mathcal{B} \setminus \overline{\mathcal{D}_{\kappa} \cup \Gamma_{\kappa}}$, observe that $\forall \Psi \in \mathbb{C}(\mathcal{B}_{\kappa}^{-})^{3 \times 3}$,

$$\begin{cases} 2\mu |\Psi|^2 \leq \Re(\Psi:C:\overline{\Psi}) \leq (3\lambda+2\mu)|\Psi|^2 & \text{for } 0<\nu<\frac{1}{2}\\ (3\lambda+2\mu)|\Psi|^2 \leq \Re(\Psi:C:\overline{\Psi}) \leq 2\mu |\Psi|^2 & \text{for } -1<\nu<0 \end{cases}, \quad \Im(\Psi:C:\overline{\Psi})=0.$$

Next, invoke $\mathcal{D}_{\kappa}^{n} \subset \mathcal{D}_{\kappa}^{*}$ with constant $(C_{\kappa}, \rho_{\kappa})$, and let c_{κ}^{n} , c_{κ}^{n} , c_{κ}^{n} , c_{κ}^{n} and V_{κ}^{n} represent the respective values of c_{κ} , c_{κ} , v_{κ} and v_{κ} in each \mathcal{D}_{κ}^{n} , $n \in \{1, \dots, N_{\kappa}^{\star}\}$ and $\kappa \in \{\circ, 1, \dots\}$. Then, in light of [46], $\forall \kappa$

$$\left(\rho < \rho_{\kappa} \ \land \ \max\{3\lambda + 2\mu, 2\mu\} < \min\{\mathfrak{c}_{\kappa}^{n}\}\right) \ \lor \ \left(\rho > \rho_{\kappa} \ \land \ \min\{3\lambda + 2\mu, 2\mu\} > \max\{\mathfrak{c}_{\kappa}^{n}\}\right).$$

(a) Experiments

The domain \mathcal{B} is subject to periodic inspections at time steps $t_{\kappa} = \{t_{\circ}, t_{1}, \ldots\}$. At every t_{κ} , the specimen is excited by a combination of ultrasonic sources on its external boundary $\partial \mathcal{B}_t$ so that the corresponding incident field $u^f \in H^1(\mathcal{B})^3$ in the baseline model is governed by

$$\begin{cases}
\nabla \cdot C : \nabla u^{f}(\xi) + \rho \omega^{2} u^{f}(\xi) = 0, & \xi \in \mathcal{B}, \\
n \cdot C : \nabla u^{f}(\xi) = \tau(\xi), & \xi \in \partial \mathcal{B}_{t}, \\
u^{f}(\xi) = 0, & \xi \in \partial \mathcal{B} \setminus \partial \mathcal{B}_{t}.
\end{cases} (2.3)$$

Here, the illumination frequency $\omega > 0$ is selected such that the shear wavelength $\lambda_s = 2\pi \sqrt{\mu/(\rho\omega^2)}$ is sufficiently smaller than the characteristic length scale of the sought-for objects; n is the unit outward normal to the sample's boundary $\partial \mathcal{B}$; $\tau(\xi)$ represents the external traction on the Neumann part of the boundary $\partial \mathcal{B}_t \subset \partial \mathcal{B}$ which includes the source input. It is assumed that $\operatorname{supp}(\partial \mathcal{B} \setminus \overline{\partial \mathcal{B}_t}) = \emptyset$, i.e. a set of fixed boundary points of zero surface measure prevent the rigid body motion. Henceforth, the homogeneous Dirichlet part of the boundary will be implicitly indicated. At every sensing step t_κ , the interaction of u^f with the hidden scatterers $\Gamma_\kappa \cup \mathcal{D}_\kappa$ gives rise to the total field $(u^\kappa, w^\kappa) \in H^1(\mathcal{B}_\kappa^-)^3 \times H^1(\mathcal{D}_\kappa^* \setminus \overline{\Gamma_\kappa})^3$ satisfying

to the total field
$$(u^{\kappa}, w^{\kappa}) \in H^{\kappa}(\mathcal{B}_{\kappa}) \times H^{\kappa}(\mathcal{D}_{\kappa} \setminus I_{\kappa})$$
 satisfying
$$\begin{cases}
\nabla \cdot C : \nabla u^{\kappa}(\xi) + \rho \omega^{2} u^{\kappa}(\xi) = 0, & \xi \in \mathcal{B}_{\kappa}^{-}, \\
\nabla \cdot [C_{\kappa}(\xi) : \nabla w^{\kappa}](\xi) + \rho_{\kappa}(\xi) \omega^{2} w^{\kappa}(\xi) = 0, & \xi \in \mathcal{D}_{\kappa}^{\star} \setminus \overline{I_{\kappa}}, \\
t[u^{\kappa}](\xi) = t[w^{\kappa}](\xi), & u^{\kappa}(\xi) = w^{\kappa}(\xi), & \xi \in \partial \mathcal{D}_{\kappa}^{\star} \setminus \overline{I_{\kappa}}, \\
t[u](\xi) = K_{\kappa}(\xi)[[u]](\xi), & [t[u]](\xi) = 0, & \xi \in \mathcal{F}_{\kappa}, \\
t[u^{\kappa}](\xi) = 0, & \xi \in \partial \mathcal{D}_{\kappa}^{0}, \\
t[u^{\kappa}](\xi) = \tau(\xi), & \xi \in \partial \mathcal{B}_{t}.
\end{cases}$$
(2.4)

Here,

$$\begin{cases} t[u^{\kappa}](\xi) = n(\xi) \cdot C : \nabla u^{\kappa}(\xi), & \xi \in \partial \mathcal{B}_t \cup \partial \mathcal{D}_{\kappa} \\ t[w^{\kappa}](\xi) = n(\xi) \cdot C_{\kappa}(\xi) : \nabla w^{\kappa}(\xi), & \xi \in \partial \mathcal{D}_{\kappa}^{\star} \end{cases}$$

where n is the unit *outward* normal to $\partial \mathcal{B}$ and $\partial \mathcal{D}_{\kappa}$. In addition, $[\![\mathbf{u}]\!]$ (*resp.* $[\![t[\mathbf{u}]]\!]$) denotes the jump in displacement \mathbf{u} (*resp.* traction $t[\mathbf{u}]$) across Γ_{κ} such that

where

$$\llbracket f \rrbracket = f^+ - f^-, \quad f^{\pm}(\xi) = \lim_{h \to 0^+} f(\xi \pm hn(\xi)), \quad \xi \in \Gamma_{\kappa}.$$

Keep in mind that the unit normal vector \mathbf{n} to Γ_{κ} is specified earlier. Also, the second of (2.4) should be understood as a shorthand for the set of N_{κ}^{\star} governing equations over the respective homogeneous regions $\mathcal{D}_{\kappa}^{n}(n=1,\ldots,N_{\kappa}^{\star})$, supplemented by the continuity and interfacial conditions for displacement and traction across $\partial \mathcal{D}_{\kappa}^{n}$ as applicable.

Assumption 2.4. $\omega > 0$ is not an eigenvalue of the homogeneous form of (2.3) and (2.4).

Given (2.3) and (2.4), the scattered field $v^{\kappa} \in H^1(\mathcal{B}_{\kappa}^- \cup \mathcal{D}_{\kappa}^{\star} \setminus \overline{\Gamma_{\kappa}})^3$ is governed by

$$\begin{cases}
\nabla \cdot C : \nabla v^{\kappa}(\xi) + \rho \omega^{2} v^{\kappa}(\xi) + \mathbb{I}(\mathcal{D}_{\kappa}^{*} \setminus \overline{\Gamma_{\kappa}})[f_{\kappa} + \nabla \cdot \sigma_{\kappa}](\xi) = 0, & \xi \in \mathcal{B}_{\kappa}^{-} \cup \mathcal{D}_{\kappa}^{*} \setminus \overline{\Gamma_{\kappa}}, \\
t[v^{\kappa}](\xi) + \mathbb{I}(\overline{\mathcal{D}_{\kappa}^{*}} \cap \Gamma_{\kappa})n \cdot \sigma_{\kappa}(\xi) = K_{\kappa}(\xi)[[v^{\kappa}]](\xi) - t^{f}(\xi), & \xi \in \Gamma_{\kappa}, \\
[t[v^{\kappa}] + \mathbb{I}(\mathcal{D}_{\kappa}^{*} \cap \Gamma_{\kappa})n \cdot \sigma_{\kappa}(\xi)](\xi) = \mathbb{I}(\partial \mathcal{D}_{\kappa}^{*} \cap \Gamma_{\kappa})n \cdot \sigma_{\kappa}(\xi), & \xi \in \partial \mathcal{D}_{\kappa}^{*} \setminus \overline{\Gamma_{\kappa}}, \\
[t[v^{\kappa}]](\xi) = n \cdot \sigma_{\kappa}(\xi), & \xi \in \partial \mathcal{D}_{\kappa}^{*} \setminus \overline{\Gamma_{\kappa}}, \\
t[v^{\kappa}](\xi) = -t^{f}(\xi), & \xi \in \partial \mathcal{D}_{\kappa}^{*}, \\
t[v^{\kappa}](\xi) = 0, & \xi \in \partial \mathcal{B}_{t},
\end{cases}$$
(2.5)

where $t^f := n \cdot C : \nabla u^f$; $t[v^{\kappa}] = t^-[v^{\kappa}] := n \cdot C : \nabla v^{\kappa^-}$; and,

$$f_{\kappa}(\boldsymbol{\xi}) := (\rho_{\kappa}(\boldsymbol{\xi}) - \rho) \omega^{2} w^{\kappa}(\boldsymbol{\xi}), \quad \sigma_{\kappa}(\boldsymbol{\xi}) := (C_{\kappa}(\boldsymbol{\xi}) - C) : \nabla w^{\kappa}(\boldsymbol{\xi}), \quad \boldsymbol{\xi} \in \mathcal{D}_{\kappa}^{\star} \setminus \overline{\Gamma_{\kappa}}.$$

(b) Dimensional platform

In what follows, all quantities are rendered dimensionless by taking ρ , μ and ℓ_{\circ} —denoting the minimum length-scale attributed to the hidden scatterers, as the respective reference scales for mass density, elastic modulus and length—which amounts to setting $\rho = \mu = \ell_{\circ} = 1$ [51].

(c) Function spaces

It is known that stress singularities at the branch points of multiple intersecting fractures in an isotropic and homogeneous background is weaker than the classical crack-tip singularity [52,53]. The latter is also the case for delamination cracks propagating along bi-material interfaces [54]. High-order singularities may occur when a crack tip meets a bi-material interface in an angle [55,56], in which case it is shown that the contact laws in the vicinity of the crack tip may be modified such that the usual asymptotic forms for stress still applies [57]. In light of this, it will be assumed that $\llbracket \mathbf{u} \rrbracket \in \tilde{H}^{1/2}(\Gamma_{\kappa})^3$ where

$$\begin{cases}
H^{\pm 1/2}(\Gamma_{\kappa})^{3} := \{f |_{\Gamma_{\kappa}} : f \in H^{\pm 1/2}(\partial D)^{3} \}, \\
\tilde{H}^{\pm 1/2}(\Gamma_{\kappa})^{3} := \{f \in H^{\pm 1/2}(\partial D)^{3} : \operatorname{supp}(f) \subset \overline{\Gamma}_{\kappa} \}.
\end{cases} (2.6)$$

Here, $D=\bigcup_{n=1}^{N_\kappa}D_n$ is a multiply connected Lipschitz domain of bounded support such that $\Gamma_\kappa\subset\partial D$. Recall that D_n is an arbitrary extension of Γ_n defined in the above. On invoking $H^{-1/2}(\Gamma_\kappa)^3$ and $\tilde{H}^{-1/2}(\Gamma_\kappa)^3$ as the respective dual spaces of $\tilde{H}^{1/2}(\Gamma_\kappa)^3$ and $H^{1/2}(\Gamma_\kappa)^3$, it follows that

$$\tilde{H}^{\frac{1}{2}}(\Gamma_{\kappa})^{3} \subset H^{\frac{1}{2}}(\Gamma_{\kappa})^{3} \subset L^{2}(\Gamma_{\kappa})^{3} \subset \tilde{H}^{-\frac{1}{2}}(\Gamma_{\kappa})^{3} \subset H^{-\frac{1}{2}}(\Gamma_{\kappa})^{3}. \tag{2.7}$$

In this setting, $t[\mathbf{u}] \in H^{-1/2}(\Gamma_{\kappa})^3$. For future reference, let us also define

$$\begin{cases} S(\mathcal{D}_{\kappa}^{\star} \cup \Gamma_{\kappa} \cup \partial \mathcal{D}_{\kappa}^{0}) := L^{2}(\mathcal{D}_{\kappa}^{\star} \setminus \overline{\Gamma_{\kappa}})^{3} \times L^{2}(\mathcal{D}_{\kappa}^{\star} \setminus \overline{\Gamma_{\kappa}})^{3 \times 3} \times H^{-\frac{1}{2}}(\Gamma_{\kappa})^{3} \times H^{-\frac{1}{2}}(\partial \mathcal{D}_{\kappa}^{0})^{3}, \\ \tilde{S}(\mathcal{D}_{\kappa}^{\star} \cup \Gamma_{\kappa} \cup \partial \mathcal{D}_{\kappa}^{0}) := L^{2}(\mathcal{D}_{\kappa}^{\star} \setminus \overline{\Gamma_{\kappa}})^{3} \times L^{2}(\mathcal{D}_{\kappa}^{\star} \setminus \overline{\Gamma_{\kappa}})^{3 \times 3} \times \tilde{H}^{\frac{1}{2}}(\Gamma_{\kappa})^{3} \times \tilde{H}^{\frac{1}{2}}(\partial \mathcal{D}_{\kappa}^{0})^{3}. \end{cases}$$

$$(2.8)$$

(d) Well-posedness

Under assumptions 2.1 and 2.2, observe that the direct scattering problem (2.5) is of Fredholm type, and thus, its well-posedness may be established by drawing from the unique continuation principles. See Appendix A for details.

(e) Scattering signatures

By deploying Betti's reciprocal theorem, one obtains the following integral representation for the scattered fields $v^{\kappa} := u^{\kappa} - u^{f}$, $\kappa = \{0, 1, 2, ...\}$, on the specimen's boundary.

$$\begin{cases}
\frac{1}{2}v^{\kappa}(\xi) = \int_{\mathcal{D}_{\kappa}^{\star}\backslash\overline{\Gamma_{\kappa}}} \left[(\rho_{\kappa}(y) - \rho)\omega^{2}w^{\kappa}(y) \cdot G(\xi, y) - \nabla G(\xi, y) : (C_{\kappa}(y) - C) : \nabla w^{\kappa}(y) \right] dV_{y} \\
+ \int_{\partial\mathcal{D}_{\kappa}^{0}} u^{\kappa}(y) \cdot T(\xi, y) dS_{y} + \int_{\Gamma_{\kappa}} \left[\left[\mathbf{u} \right] \right] (y) \cdot T(\xi, y) dS_{y}, \\
T(\xi, y) := n(y) \cdot \Sigma(\xi, y), \quad \xi \in \partial \mathcal{B}_{t}.
\end{cases} (2.9)$$

Here, $G(\xi, y)$ is Green's displacement tensor solving

$$\begin{cases}
\nabla_{y} \cdot C : \nabla_{y} G(\xi, y) + \rho \omega^{2} G(\xi, y) + \delta(y - \xi) I_{3 \times 3} = \mathbf{0}, & y \in \mathcal{B} \setminus \{\xi\}, \\
\mathbf{n} \cdot C : \nabla_{y} G(\xi, y) = \mathbf{0}, & y \in \partial \mathcal{B}_{t},
\end{cases} (2.10)$$

and $\Sigma(\xi, y) := C : \nabla_y G(\xi, y)$ is the associated Green's stress tensor.

3. Scattering operators

Let us define the scattering operator $\Lambda_{\kappa}: L^2(\partial \mathcal{B}_t)^3 \to L^2(\partial \mathcal{B}_t)^3$ by

$$\Lambda_{\kappa}(\tau) = v^{\kappa} \big|_{\partial \mathcal{B}_{\kappa'}} \quad \kappa = 0, 1, 2, \dots, \tag{3.1}$$

where v^{κ} solves (2.5). Then, there exists the factorization

$$\Lambda_{\kappa} = \mathcal{S}_{\kappa}^* T_{\kappa} \mathcal{S}_{\kappa}, \tag{3.2}$$

such that $S_{\kappa}: L^2(\partial \mathcal{B}_t)^3 \to S(\mathcal{D}_{\kappa}^{\star} \cup \Gamma_{\kappa} \cup \partial \mathcal{D}_{\kappa}^0)$ is defined by

$$S_{\kappa}(\tau) := \left(u^{f} \big|_{\mathcal{D}_{\kappa}^{+} \setminus \overline{\Gamma_{\kappa}}'}, \nabla u^{f} \big|_{\mathcal{D}_{\kappa}^{+} \setminus \overline{\Gamma_{\kappa}}'}, t[u^{f}] \big|_{\Gamma_{\kappa}'}, t[u^{f}] \big|_{\partial \mathcal{D}_{\kappa}^{0}} \right), \tag{3.3}$$

whose adjoint operator $S_{\kappa}^* : \tilde{S}(\mathcal{D}_{\kappa}^* \cup \Gamma_{\kappa} \cup \partial \mathcal{D}_{\kappa}^0) \to L^2(\partial \mathcal{B}_t)^3$ takes the form

$$S_{\kappa}^{*}(\boldsymbol{\phi}, \boldsymbol{\Phi}, \boldsymbol{\varphi}, \boldsymbol{\phi}) := \boldsymbol{v}^{*}(\boldsymbol{\xi}), \quad \boldsymbol{\xi} \in \partial \mathcal{B}_{t}, \tag{3.4}$$

where $\mathbf{v}^* \in H^1(\mathcal{B} \setminus \overline{\Gamma_{\kappa} \cup \partial \mathcal{D}_{\kappa}})^3$ solves

$$\begin{cases}
\nabla \cdot C : \nabla v^{*}(\xi) + \rho \omega^{2} v^{*}(\xi) \\
+ \mathbb{1}(\mathcal{D}_{\kappa}^{*} \setminus \overline{\Gamma_{\kappa}})(\phi - \nabla \cdot \Phi) = 0, & \xi \in \mathcal{B} \setminus \overline{\Gamma_{\kappa}} \cup \partial \overline{\mathcal{D}_{\kappa}}, \\
\llbracket t[v^{*}] \rrbracket(\xi) = -n \cdot \Phi(\xi), & \llbracket v^{*} \rrbracket(\xi) = 0, & \xi \in \partial \mathcal{D}_{\kappa}^{*} \setminus \overline{\Gamma_{\kappa}}, \\
\llbracket v^{*} \rrbracket(\xi) = \varphi, & \llbracket t[v^{*}] - \mathbb{1}(\mathcal{D}_{\kappa}^{*} \cap \Gamma_{\kappa})n \cdot \Phi \rrbracket(\xi) & \xi \in \partial \mathcal{D}_{\kappa}^{*} \setminus \overline{\Gamma_{\kappa}}, \\
= -\mathbb{1}(\partial \mathcal{D}_{\kappa}^{*} \cap \Gamma_{\kappa})n \cdot \Phi(\xi), & \xi \in \partial \mathcal{D}_{\kappa}^{0}, \\
\llbracket v^{*} \rrbracket(\xi) = \varphi, & \llbracket t[v^{*}] \rrbracket(\xi) = 0 & \xi \in \partial \mathcal{D}_{\kappa}^{0}, \\
t[v^{*}](\xi) = 0, & \xi \in \partial \mathcal{B}_{t},
\end{cases}$$
(3.5)

wherein $t[v^*] := n \cdot C : \nabla v^*$. This may be observed by (i) pre-multiplying the first of (3.5) by \bar{u}^f and (ii) post-multiplying the conjugated first of (2.3) by v^* . Integration by parts over $\mathcal{B} \setminus \overline{\Gamma_{\kappa} \cup \partial \mathcal{D}_{\kappa}}$ followed by application of the contact condition over $\Gamma_{\kappa} \cup \partial \mathcal{D}_{\kappa}$ and summation of the results yield

$$\begin{split} \int_{\partial \mathcal{B}_t} \bar{\boldsymbol{\tau}} \cdot \boldsymbol{v}^* \, \mathrm{d}S_{\boldsymbol{\xi}} &= \int_{\mathcal{D}_{\boldsymbol{\kappa}}^* \setminus \overline{\Gamma_{\boldsymbol{\kappa}}}} \left(\bar{\boldsymbol{u}}^\mathrm{f} \cdot \boldsymbol{\Phi} + \nabla \bar{\boldsymbol{u}}^\mathrm{f} : \boldsymbol{\varPhi} \right) \mathrm{d}V_{\boldsymbol{\xi}} \\ &+ \int_{\Gamma_{\boldsymbol{\kappa}}} \bar{\boldsymbol{t}} [\boldsymbol{u}^\mathrm{f}] \cdot \boldsymbol{\varphi} \, \mathrm{d}S_{\boldsymbol{\xi}} + \int_{\partial \mathcal{D}_{\boldsymbol{\kappa}}^0} \bar{\boldsymbol{t}} [\boldsymbol{u}^\mathrm{f}] \cdot \boldsymbol{\varphi} \, \mathrm{d}S_{\boldsymbol{\xi}}, \end{split}$$

which substantiates (3.4) via $\langle (\phi, \Phi, \varphi, \phi), \mathcal{S}_{\kappa}(\tau) \rangle_{\mathcal{D}_{\kappa}^{*} \cup \Gamma_{\kappa} \cup \partial \mathcal{D}_{\kappa}^{o}} = \langle v^{*}, \tau \rangle_{\partial \mathcal{B}_{t}}$. Here,

$$\begin{cases}
\langle \cdot, \cdot \rangle_{\mathcal{D}_{\kappa}^{\star} \cup \Gamma_{\kappa} \cup \partial \mathcal{D}_{\kappa}^{o}} := \langle \tilde{S}(\mathcal{D}_{\kappa}^{\star} \cup \Gamma_{\kappa} \cup \partial \mathcal{D}_{\kappa}^{o}), S(\mathcal{D}_{\kappa}^{\star} \cup \Gamma_{\kappa} \cup \partial \mathcal{D}_{\kappa}^{o}) \rangle, \\
\langle \cdot, \cdot \rangle_{\partial \mathcal{B}_{t}} := \langle \tilde{H}^{\frac{1}{2}}(\partial \mathcal{B}_{t})^{3}, H^{-\frac{1}{2}}(\partial \mathcal{B}_{t})^{3} \rangle,
\end{cases} (3.6)$$

extend L^2 inner products. In this setting, the middle operator $T_{\kappa}: S(\mathcal{D}_{\kappa}^{\star} \cup \Gamma_{\kappa} \cup \partial \mathcal{D}_{\kappa}^{o}) \to \tilde{S}(\mathcal{D}_{\kappa}^{\star} \cup \Gamma_{\kappa} \cup \partial \mathcal{D}_{\kappa}^{o})$ is given by

$$T_{\kappa}\left(u^{f}\big|_{\mathcal{D}_{\kappa}^{\star}\setminus\overline{\Gamma_{\kappa}}}, \nabla u^{f}\big|_{\mathcal{D}_{\kappa}^{\star}\setminus\overline{\Gamma_{\kappa}}}, t[u^{f}]\big|_{\Gamma_{\kappa}}, t[u^{f}]\big|_{\partial\mathcal{D}_{\kappa}^{0}}\right)$$

$$:=\left((\rho_{\kappa}-\rho)\omega^{2}w^{\kappa}\big|_{\mathcal{D}_{\kappa}^{\star}\setminus\overline{\Gamma_{\kappa}}}, -(C_{\kappa}-C): \nabla w^{\kappa}\big|_{\mathcal{D}_{\kappa}^{\star}\setminus\overline{\Gamma_{\kappa}}}, \left[\left[\mathbf{u}\right]\right]\big|_{\Gamma_{\kappa}}, u^{\kappa}\big|_{\partial\mathcal{D}_{\nu}^{0}}\right). \tag{3.7}$$

4. Properties of operators

Assumption 4.1. Given $\kappa \in \{\circ, 1, ...\}$ and $j \in \{\circ, 1, ..., N_{\kappa}^{o}\}$, suppose that (a) \mathcal{D}_{κ}^{o} may be decomposed into simply connected components $\mathcal{D}_{\kappa,j}^{o} \subset \mathcal{D}_{\kappa}^{o}$, and (b) Γ_{κ} consists of $M_{\kappa} \geq 1$ (possibly disjoint) analytic surfaces $S_{m} \subset \Gamma_{\kappa}$, $m = 1, ..., M_{\kappa}$, with the unique continuation ∂D_{m} identifying the 'interior' domain $D_{m} \subset \mathcal{B}$. Then for any j (resp. m), it is assumed that $\omega > 0$ is not a

'Neumann' eigenfrequency of the Navier equation in $\mathcal{D}^o_{\kappa,j}$ (resp. D_m), i.e. as long as $\mathbf{u}_j \in H^1(\mathcal{D}^o_{\kappa,j})^3$ and $\mathbf{u}_m \in H^1(D_m)^3$ satisfying

$$\begin{cases} \nabla \cdot (C : \nabla \mathbf{u}_{j}) + \rho \,\omega^{2} \mathbf{u}_{j} = \mathbf{0} & \text{in } \mathcal{D}_{\kappa,j}^{0} \\ \mathbf{n} \cdot C : \nabla \mathbf{u}_{j} = \mathbf{0} & \text{on } \partial \mathcal{D}_{\kappa,j}^{0} \end{cases} \wedge \begin{cases} \nabla \cdot (C_{\kappa} : \nabla \mathbf{u}_{m}) + \rho_{\kappa} \,\omega^{2} \mathbf{u}_{m} = \mathbf{0} & \text{in } \mathbf{D}_{m} \\ \mathbf{n} \cdot C_{\kappa} : \nabla \mathbf{u}_{m} = \mathbf{0} & \text{on } \partial \mathbf{D}_{m} \end{cases}$$
(4.1)

vanish identically in $\mathcal{D}_{\kappa,j}^{o}$ and \mathfrak{d}_{m} , respectively. If \mathfrak{d}_{m} is bounded, the real eigenfrequencies of (4.1) form a discrete set [46,47].

Lemma 4.2. In light of the unique continuation principle, the operator $S_{\kappa}: L^2(\partial \mathcal{B}_t)^3 \to S(\mathcal{D}_{\kappa}^{\star} \cup \Gamma_{\kappa} \cup \partial \mathcal{D}_{\kappa}^0)$ is injective at all t_{κ} .

Lemma 4.3. Let

$$H_{\Delta} = \{\hat{\mathbf{u}} \in H^{1}(\mathcal{D}_{\kappa}^{\star})^{3} \mid \nabla \cdot \mathbf{C} : \nabla \hat{\mathbf{u}} + \rho \,\omega^{2} \hat{\mathbf{u}} = \mathbf{0} \text{ in } \mathcal{D}_{\kappa}^{\star}\},$$

and define the map $(\hat{S}_1, \hat{S}_2, \hat{S}_3) : H_{\Delta} \to L^2(\mathcal{D}_{\kappa}^{\star} \setminus \overline{\Gamma_{\kappa}})^3 \times L^2(\mathcal{D}_{\kappa}^{\star} \setminus \overline{\Gamma_{\kappa}})^{3 \times 3} \times L^2(\Gamma_{\kappa} \cap \overline{\mathcal{D}_{\kappa}^{\star}})^3$ such that

$$(\hat{S}_1, \hat{S}_2, \hat{S}_3)(\hat{\mathbf{u}}) = (\hat{\mathbf{u}}|_{\mathcal{D}_{\nu}^{\star} \setminus \overline{\Gamma_{\kappa}}}, \nabla \hat{\mathbf{u}}|_{\mathcal{D}_{\nu}^{\star} \setminus \overline{\Gamma_{\kappa}}}, t[\hat{\mathbf{u}}]|_{\Gamma_{\kappa} \cap \overline{\mathcal{D}_{\nu}^{\star}}}), \quad t[\hat{\mathbf{u}}] = n \cdot C : \nabla \hat{\mathbf{u}},$$

then $\mathfrak{S}(H_{\Delta}) := \hat{S}_1(H_{\Delta}) \times \hat{S}_2(H_{\Delta}) \times (\hat{S}_3(H_{\Delta}) \oplus H^{-1/2}(\Gamma_{\kappa} \setminus \overline{\mathcal{D}_{\kappa}^{\star}})^3) \times H^{-1/2}(\partial \mathcal{D}_{\kappa}^0)^3 = \overline{\mathcal{R}(\mathcal{S}_{\kappa})}$ where the latter denotes the closure of the range of \mathcal{S}_{κ} .

Proof. Observe that the restriction of $u^f \in H^1(\mathcal{B})^3$, satisfying (2.3), to $\mathcal{D}_{\kappa}^{\star}$ belongs to H_{Δ} , hence $\mathcal{R}(\mathcal{S}_{\kappa}) \subset \mathfrak{S}(H_{\Delta})$. To prove the claim, it is then sufficient to establish that $\mathcal{S}_{\kappa}^{\star} : \mathfrak{S}(H_{\Delta}) \to L^2(\partial \mathcal{B}_t)^3$ given by

$$\frac{1}{2} \mathcal{S}_{\kappa}^{*}(\boldsymbol{\Phi}, \boldsymbol{\varPhi}, \boldsymbol{\varphi} \oplus \boldsymbol{\psi}, \boldsymbol{\phi}) = \int_{\mathcal{D}_{\kappa}^{*} \setminus \overline{\Gamma_{\kappa}}} \left[\boldsymbol{\Phi}(\boldsymbol{y}) \cdot \boldsymbol{G}(\boldsymbol{\xi}, \boldsymbol{y}) + \boldsymbol{\varPhi}(\boldsymbol{y}) : \nabla \boldsymbol{G}(\boldsymbol{\xi}, \boldsymbol{y}) \right] dV_{\boldsymbol{y}}
+ \int_{\Gamma_{\kappa} \cap \overline{\mathcal{D}_{\kappa}^{*}}} \boldsymbol{\varphi}(\boldsymbol{y}) \cdot \boldsymbol{T}(\boldsymbol{\xi}, \boldsymbol{y}) dS_{\boldsymbol{y}} + \int_{\Gamma_{\kappa} \setminus \overline{\mathcal{D}_{\kappa}^{*}}} \boldsymbol{\psi}(\boldsymbol{y}) \cdot \boldsymbol{T}(\boldsymbol{\xi}, \boldsymbol{y}) dS_{\boldsymbol{y}}
+ \int_{\partial \mathcal{D}_{\kappa}^{0}} \boldsymbol{\phi}(\boldsymbol{y}) \cdot \boldsymbol{T}(\boldsymbol{\xi}, \boldsymbol{y}) dS_{\boldsymbol{y}},$$
(4.2)

is injective on $\mathfrak{S}(H_{\Delta})$. Suppose that there exists $(\phi, \Phi, \varphi \oplus \psi, \phi) = (\mathbf{u}^i, \nabla \mathbf{u}^i, \mathbf{t}[\mathbf{u}^i] \oplus \psi, \phi)$ —with $\mathbf{u}^i \in H^1(\mathcal{D}_{\kappa}^*)^3$ satisfying $\nabla \cdot C : \nabla \mathbf{u}^i + \rho \, \omega^2 \mathbf{u}^i = \mathbf{0}$ in \mathcal{D}_{κ}^* while $(\psi, \phi) \in \tilde{H}^{1/2}(\Gamma_{\kappa} \setminus \overline{\mathcal{D}_{\kappa}^*})^3 \times \tilde{H}^{1/2}(\partial \mathcal{D}_{\kappa}^0)^3$ —such that $\mathcal{S}_{\kappa}^*(\mathbf{u}^i, \nabla \mathbf{u}^i, \mathbf{t}[\mathbf{u}^i] \oplus \psi, \phi) = \mathbf{0}$. Since by construction $\mathbf{v}^{\kappa}(\xi) = \mathcal{S}_{\kappa}^*(\cdot)$ on $\xi \in \partial \mathcal{B}_t$, it is evident from (2.5) that \mathbf{v}^{κ} has trivial Dirichlet and Neumann traces on $\partial \mathcal{B}_t$, and thus, the unique continuation principle reads $\mathbf{v}^{\kappa} = \mathbf{0}$ in $\mathcal{B} \setminus \overline{\Gamma_{\kappa}} \cup \overline{\mathcal{D}_{\kappa}}$. From (a) properties of the layer potentials, i.e. $\phi = \mathbf{u}^{\kappa}$ and $\psi = [\![\mathbf{v}^{\kappa}]\!]$, (b) fifth of (2.5) which reads $\mathbf{t}^f = \mathbf{0}$ on $\partial \mathcal{D}_{\kappa}^0$, and (c) assumption 4.1 indicating that $\omega > 0$ is not a Neumann eigenfrequency of the Navier equation affiliated with any simply connected subset of \mathcal{D}_{κ}^0 , one may conclude that $\psi = \phi = \mathbf{0}$. Now, on denoting $\Gamma_{\kappa}^t = \Gamma_{\kappa} \cap \overline{\mathcal{D}_{\kappa}^*}$ and $\mathcal{B}^* = \mathcal{B} \setminus \overline{\Gamma_{\kappa}^t} \cup \partial \mathcal{D}_{\kappa}^*$, let $\forall \xi \in \mathcal{B} \setminus \overline{\Gamma_{\kappa}^t}$,

$$\mathbf{v}(\boldsymbol{\xi}) = \int_{\mathcal{D}_{\kappa}^{\star} \setminus \overline{I_{\kappa}}} \left[\mathbf{u}^{i}(y) \cdot G(\boldsymbol{\xi}, y) + \nabla \mathbf{u}^{i}(y) : \nabla G(\boldsymbol{\xi}, y) \right] dV_{y}$$

$$+ \int_{I_{\kappa}^{+}} t \left[\mathbf{u}^{i} \right](y) \cdot T(\boldsymbol{\xi}, y) dS_{y}.$$

$$(4.3)$$

From the regularity of volume potentials, one may infer that $\forall \mathbf{v}' \in H^1(\mathcal{B}^*)$, $\mathbf{v} \in H^1(\mathcal{B}^*)$ satisfies

$$\int_{\mathcal{B}_{\star}} \left[\rho \, \omega^{2} \, \mathbf{v}' \cdot \mathbf{v} - \nabla \, \mathbf{v}' : C : \nabla \mathbf{v} \right] dV_{\xi} - \int_{\Gamma_{\kappa}^{i}} \left[\mathbf{v}' \right] \cdot (\mathbf{n} \cdot \left[C : \nabla \mathbf{v} - \nabla \mathbf{u}^{i} \right]) dS_{\xi}
= -\int_{\mathcal{D}_{\star}^{\star} \setminus \overline{\Gamma_{\kappa}}} \left[\mathbf{v}' \cdot \mathbf{u}^{i} + \nabla \, \mathbf{v}' : \nabla \mathbf{u}^{i} \right] dV_{\xi}.$$
(4.4)

Note that $\mathbf{v} = \mathcal{S}_{\kappa}^*(\mathbf{u}^i, \nabla \mathbf{u}^i, t[\mathbf{u}^i] \oplus 0, 0)$ on $\partial \mathcal{B}_t$, then $\mathcal{S}_{\kappa}^*(\cdot) = \mathbf{0}$ implies that $\mathbf{v} = \mathbf{0}$ in $\mathcal{B}^* \setminus \overline{\mathcal{D}_{\kappa}^*}$. Then by setting $\mathbf{v}' = \bar{\mathbf{u}}^i$, (4.4) may be recast as

$$\int_{\mathcal{D}_{\nu}^{\star}\backslash\overline{\Gamma_{\kappa}}} \left[\rho \,\omega^{2} \,\bar{\mathbf{u}}^{i} \cdot \mathbf{v} - \nabla \,\bar{\mathbf{u}}^{i} : C : \nabla \mathbf{v}\right] \mathrm{d}V_{\xi} = - \|\,\mathbf{u}^{i}\,\|_{H^{1}(\mathcal{D}_{\kappa}^{\star}\backslash\overline{\Gamma_{\kappa}})^{3}}^{2}. \tag{4.5}$$

Also, on recalling $\nabla \cdot \mathbf{C} : \nabla \mathbf{u}^i + \rho \, \omega^2 \mathbf{u}^i = \mathbf{0}$ in $\mathcal{D}_{\kappa}^{\star}$, it follows that

$$\int_{\mathcal{D}_{c}^{+} \setminus \overline{\Gamma_{k}}} \left[\rho \, \omega^{2} \, \bar{\mathbf{u}}^{i} \cdot \mathbf{v} - \nabla \, \bar{\mathbf{u}}^{i} : C : \nabla \mathbf{v} \right] dV_{\xi} = \| \mathbf{t} [\mathbf{u}^{i}] \|_{L^{2}(\Gamma_{k}^{i})^{3}}^{2}. \tag{4.6}$$

Combining (4.5) and (4.6) reads $(\phi, \Phi, \varphi) = 0$ which completes the proof.

Lemma 4.4. Under assumption 2.2, the operator $S_{\kappa}^* : \tilde{S}(\mathcal{D}_{\kappa}^{\star} \cup \Gamma_{\kappa} \cup \partial \mathcal{D}_{\kappa}^{o}) \to L^2(\partial \mathcal{B}_t)^3$ is compact and has a dense range.

Proof. The compactness of S_{κ}^* is established by the smooth kernels in its integral form (4.2), and its dense range results from the injectivity of S_{κ} per lemma 4.2.

Assumption 4.5. Under assumptions 2.1–2.3, given $(\mathbf{f}^{\kappa}, \mathbf{g}^{\kappa}) \in H^{-1/2}(\partial \mathcal{D}_{\kappa}^{\star})^3 \times H^{1/2}(\partial \mathcal{D}_{\kappa}^{\star})^3$, consider the solution $(\mathbf{u}^{\kappa}, \mathbf{w}^{\kappa}) \in H^1(\mathcal{D}_{\kappa}^{\star})^3 \times H^1(\mathcal{D}_{\kappa}^{\star})^3$ to the interior transmission problem (ITP)

$$\mathrm{ITP}(\mathcal{D}_{\kappa}^{\star}, \Gamma_{\kappa}; \{C, \rho\}, \{C_{\kappa}, \rho_{\kappa}\}, K_{\kappa}; \mathbf{f}^{\kappa}, \mathbf{g}^{\kappa})$$

$$\begin{cases}
\nabla \cdot [C_{\kappa}(\xi) : \nabla \mathbf{w}^{\kappa}](\xi) + \rho_{\kappa}(\xi) \omega^{2} \mathbf{w}^{\kappa}(\xi) = \mathbf{0}, & \xi \in \mathcal{D}_{\kappa}^{*} \setminus \overline{\Gamma_{\kappa}}, \\
\nabla \cdot C : \nabla \mathbf{u}^{\kappa}(\xi) + \rho \omega^{2} \mathbf{u}^{\kappa}(\xi) = \mathbf{0}, & \xi \in \mathcal{D}_{\kappa}^{*}, \\
t[\mathbf{w}^{\kappa}](\xi) - t[\mathbf{u}^{\kappa}](\xi) = \mathbf{f}^{\kappa}(\xi), & [\mathbf{w}^{\kappa} - \mathbf{u}^{\kappa}](\xi) = \mathbf{g}^{\kappa}(\xi), & \xi \in \partial \mathcal{D}_{\kappa}^{*} \setminus \overline{\Gamma_{\kappa}}, \\
t[\mathbf{w}^{\kappa}](\xi) = K_{\kappa}(\xi)[[\mathbf{w}^{\kappa}]](\xi), & [[t[\mathbf{w}^{\kappa}]](\xi) = \mathbf{0}, & \xi \in \Gamma_{\kappa} \cap \mathcal{D}_{\kappa}^{*}, \\
t[\mathbf{w}^{\kappa}](\xi) - t[\mathbf{u}^{\kappa}](\xi) = \mathbf{f}^{\kappa}(\xi), & t[\mathbf{w}^{\kappa}](\xi) = K_{\kappa}(\xi)[\mathbf{g}^{\kappa} + \mathbf{u}^{\kappa} - \mathbf{w}^{\kappa}](\xi), & \xi \in \Gamma_{\kappa} \cap \partial \mathcal{D}_{\kappa}^{*},
\end{cases} (4.7)$$

wherein

Downloaded from https://royalsocietypublishing.org/ on 04 June 2023

$$t[\mathbf{u}^{\kappa}](\xi) = n(\xi) \cdot C : \nabla \mathbf{u}^{\kappa}(\xi), \quad t[\mathbf{w}^{\kappa}](\xi) = n(\xi) \cdot C_{\kappa}(\xi) : \nabla \mathbf{w}^{\kappa}(\xi), \quad \xi \in \Gamma_{\kappa} \cup \partial \mathcal{D}_{\kappa}^{\star}.$$

It is assumed that $\forall t_{\kappa}$, ω is such that (4.7) remains well-posed, i.e. for $(\mathbf{f}^{\kappa}, \mathbf{g}^{\kappa}) = \mathbf{0}$, the ITP does not admit a nontrivial solution $(\mathbf{u}^{\kappa}, \mathbf{w}^{\kappa})$. For $\Gamma_{\kappa} = \emptyset$, the elastodynamics ITP, with varying restrictions on C and $C_{\kappa}(\xi)$, is analysed in [42,46–48] following the variational method introduced by Hähner [58]. In the most general case, under assumptions 2.2 and 2.3, (4.7) with $\Gamma_{\kappa} = \emptyset$ is well-posed when ω does not belong to (at most) a countable set of transmission eigenvalues [46]. The latter is also concluded in a recent study of acoustic ITP for penetrable obstacles with sound-hard cracks [39]. Similar analysis could be applied to (4.7) which is beyond the scope of the present study.

Lemma 4.6. Operator $T_{\kappa}:\mathfrak{S}(H_{\Delta})\to \tilde{S}(\mathcal{D}_{\kappa}^{\star}\cup\Gamma_{\kappa}\cup\partial\mathcal{D}_{\kappa}^{0})$ in (3.7) is bounded and satisfies

$$\Im \langle T_{\kappa} \Xi, \Xi \rangle_{\mathcal{D}_{\kappa}^{\star} \cup \Gamma_{\kappa} \cup \partial \mathcal{D}_{\kappa}^{0}} > 0, \tag{4.8}$$

 $\forall \Xi \in \mathfrak{S}(H_{\Delta}) : \Xi \neq \mathbf{0}$. Consequently, T_{κ} is also injective provided that ω is not a transmission eigenvalue of (4.7) per assumption 4.5.

Proof. The well-posedness of (2.5) establishes the boundedness of T_{κ} . Now, consider v^{κ} satisfying (A 1) with $(u^{\mathrm{f}}|_{\mathcal{D}_{\kappa}^{\star}\setminus\overline{\Gamma_{\kappa}}}, \nabla u^{\mathrm{f}}|_{\mathcal{D}_{\kappa}^{\star}\setminus\overline{\Gamma_{\kappa}}}, t[u^{\mathrm{f}}]|_{\Gamma_{\kappa}}, t[u^{\mathrm{f}}]|_{\partial\mathcal{D}_{\kappa}^{o}}) = \mathcal{Z}$. Taking $v' = v^{\kappa}$ in \mathcal{B}_{κ}^{-} and $v' = w^{\kappa} - u^{\mathrm{f}}$ in $\mathcal{D}_{\kappa}^{\star}\setminus\overline{\Gamma_{\kappa}}$, observe from (A 1) that

$$\Im \langle T_{\kappa} \boldsymbol{\Xi}, \boldsymbol{\Xi} \rangle_{\mathcal{D}_{\kappa}^{\bullet} \cup \Gamma_{\kappa} \cup \partial \mathcal{D}_{\kappa}^{o}} = -\Im \left(\int_{\mathcal{D}_{\kappa}^{\bullet} \setminus \overline{\Gamma_{\kappa}}} \nabla \bar{\boldsymbol{w}}^{\kappa} : \boldsymbol{C}_{\kappa} : \nabla \boldsymbol{w}^{\kappa} \, dV_{\boldsymbol{\xi}} + \int_{\Gamma_{\kappa}} \llbracket \bar{\boldsymbol{v}}^{\kappa} \rrbracket \cdot \boldsymbol{K}_{\kappa} \llbracket \boldsymbol{v}^{\kappa} \rrbracket \, dS_{\boldsymbol{\xi}} \right), \tag{4.9}$$

whereby (4.8) follows immediately from assumption 2.2. Now, let $T_{\kappa} \Xi = 0$, then (4.9), second of (2.4), the unique continuation principle, and (2.9) imply that $S_{\kappa}^* T_{\kappa} \Xi = 0$. Then, lemma 4.7 reads $\Xi = 0$ which proves the injectivity of T_{κ} .

Lemma 4.7. Under assumption 4.5, the operator $V_{\kappa} = S_{\kappa}^* T_{\kappa} : \mathfrak{S}(H_{\Delta}) \to L^2(\partial \mathcal{B}_t)^3$ is compact and injective with dense range.

Proof. Compactness of \mathcal{V}_{κ} follows immediately from lemmas 4.4 and 4.6 which respectively establish the compactness of \mathcal{S}_{κ}^* and the boundedness of T_{κ} . To demonstrate the injectivity of \mathcal{V}_{κ} , let

$$\left(\hat{\mathbf{u}}\big|_{\mathcal{D}_{\kappa}^{*}\setminus\overline{\varGamma_{\kappa}}},\nabla\hat{\mathbf{u}}\big|_{\mathcal{D}_{\kappa}^{*}\setminus\overline{\varGamma_{\kappa}}},t[\hat{\mathbf{u}}]\big|_{\varGamma_{\kappa}\cap\overline{\mathcal{D}_{\kappa}^{*}}}\oplus\psi,\phi\right)\in\mathfrak{S}(H_{\Delta}),\ (\psi,\phi)\in H^{-1/2}(\varGamma_{\kappa}\setminus\overline{\mathcal{D}_{\kappa}^{*}})^{3}\times H^{-1/2}(\partial\mathcal{D}_{\kappa}^{0})^{3},$$

such that $\mathcal{V}_{\kappa}(\hat{\mathbf{u}}|_{\mathcal{D}_{\kappa}^{\star}\setminus\overline{\Gamma_{\kappa}}}, \nabla\hat{\mathbf{u}}|_{\mathcal{D}_{\kappa}^{\star}\setminus\overline{\Gamma_{\kappa}}}, t[\hat{\mathbf{u}}]|_{\Gamma_{\kappa}\cap\overline{\mathcal{D}_{\kappa}^{\star}}} \oplus \psi, \phi) = \mathbf{0}$. Since by definition $v^{\kappa} = \mathcal{V}_{\kappa}(\cdot)$ on $\partial\mathcal{B}_{t}$, one may observe that v^{κ} satisfying (2.5) has trivial Dirichlet and Neumann traces on $\partial\mathcal{B}_{t}$ so that by the unique continuation principle $v^{\kappa} = \mathbf{0}$ in \mathcal{B}_{κ}^{-} . Now, from (a) second and fifth of (2.5), and (b) assumption 4.1 indicating that $\omega > 0$ is not a Neumann eigenfrequency of the Navier equation affiliated with any simply connected subset of \mathcal{D}_{κ}^{0} , one may conclude that $\psi = \phi = \mathbf{0}$. Next, let us define \mathbf{w}^{κ} such that $\mathbf{w}^{\kappa} = \hat{\mathbf{u}} + \mathbf{v}^{\kappa}$ in $\mathcal{D}_{\kappa}^{\star}$, then the pair $(\hat{\mathbf{u}}, \mathbf{w}^{\kappa})$ satisfies the ITP (4.7) with trivial boundary potentials i.e., $(\mathbf{f}^{\kappa}, \mathbf{g}^{\kappa}) = \mathbf{0}$. Since ω is not a transmission eigenvalue as per assumption 4.5, one may deduce that $\hat{\mathbf{u}} = \mathbf{0}$ in $\mathcal{D}_{\kappa}^{\star} \setminus \overline{\Gamma_{\kappa}}$. Subsequently, $\nabla \hat{\mathbf{u}} = \mathbf{0}$ in $\mathcal{D}_{\kappa}^{\star} \setminus \overline{\Gamma_{\kappa}}$, and $\mathbf{t}[\hat{\mathbf{u}}] = \mathbf{0}$ on $\Gamma_{\kappa} \cap \overline{\mathcal{D}_{\kappa}^{\star}}$ which proves the injectivity of \mathcal{V}_{κ} .

Denseness of the range of \mathcal{V}_{κ} may be established by showing that the adjoint operator \mathcal{V}_{κ}^* is injective. In this vein, from definition, $\mathcal{V}_{\kappa}^*: L^2(\partial \mathcal{B}_t)^3 \to \tilde{S}(\mathcal{D}_{\kappa}^* \cup \Gamma_{\kappa} \cup \partial \mathcal{D}_{\kappa}^0)$ is given by

$$\mathcal{V}_{\kappa}^{*}(\tau) = \left((\rho_{\kappa} - \rho)\omega^{2} u^{\tau} \big|_{\mathcal{D}_{\kappa}^{+} \setminus \overline{\Gamma_{\kappa}}}, -(\overline{C_{\kappa}} - C) : \nabla u^{\tau} \big|_{\mathcal{D}_{\kappa}^{+} \setminus \overline{\Gamma_{\kappa}}}, \|u^{\tau}\|_{\Gamma_{\kappa}}, u^{\tau} \big|_{\partial \mathcal{D}_{\kappa}^{0}} \right), \tag{4.10}$$

where $u^{\tau} \in H^1(\mathcal{B}_{\kappa}^- \cup \mathcal{D}_{\kappa}^{\star} \setminus \overline{\Gamma_{\kappa}})^3$ solves

$$\begin{cases}
\nabla \cdot C : \nabla u^{\tau}(\xi) + \rho \omega^{2} u^{\tau}(\xi) + \mathbb{I}(\mathcal{D}_{\kappa}^{*} \setminus \overline{\Gamma_{\kappa}})[\mathbf{f}^{\tau} + \nabla \cdot \sigma^{\tau}](\xi) = 0, & \xi \in \mathcal{B}_{\kappa}^{-} \cup \mathcal{D}_{\kappa}^{*} \setminus \overline{\Gamma_{\kappa}}, \\
t[u^{\tau}](\xi) + \mathbb{I}(\overline{\mathcal{D}_{\kappa}^{*}} \cap \Gamma_{\kappa}) n \cdot \sigma^{\tau}(\xi) = \overline{K_{\kappa}}(\xi)[[u^{\tau}]](\xi), & \xi \in \Gamma_{\kappa}, \\
[t[u^{\tau}]] + \mathbb{I}(\mathcal{D}_{\kappa}^{*} \cap \Gamma_{\kappa}) n \cdot \sigma^{\tau}(\xi)[(\xi) = \mathbb{I}(\partial \mathcal{D}_{\kappa}^{*} \cap \Gamma_{\kappa}) n \cdot \sigma^{\tau}(\xi), & \xi \in \partial \mathcal{D}_{\kappa}^{*} \setminus \overline{\Gamma_{\kappa}}, \\
t[u^{\tau}]](\xi) = n \cdot \sigma^{\tau}(\xi), & \xi \in \partial \mathcal{D}_{\kappa}^{0}, \\
t[u^{\tau}](\xi) = 0, & \xi \in \partial \mathcal{B}_{t},
\end{cases}$$

$$(4.11)$$

where $t[u^{\tau}] := n \cdot C : \nabla u^{\tau}$, and

Downloaded from https://royalsocietypublishing.org/ on 04 June 2023

$$\mathbf{f}^{\tau}(\boldsymbol{\xi}) := (\rho_{\kappa}(\boldsymbol{\xi}) - \rho) \omega^{2} u^{\tau}(\boldsymbol{\xi}), \qquad \sigma^{\tau}(\boldsymbol{\xi}) := (\overline{C_{\kappa}}(\boldsymbol{\xi}) - C) : \nabla u^{\tau}(\boldsymbol{\xi}), \qquad \boldsymbol{\xi} \in \mathcal{D}_{\kappa}^{\star} \setminus \overline{T_{\kappa}}.$$

This may be observed by (i) pre-multiplying the first of (2.5) by $\overline{u^{\tau}}$, and (ii) post-multiplying the conjugated first of (4.11) by v^{κ} . Integration by parts over $\mathcal{B}_{\kappa}^{-} \cup \mathcal{D}_{\kappa}^{\star} \setminus \overline{\Gamma_{\kappa}}$ followed by application of the contact condition over $\Gamma_{\kappa} \cup \partial \mathcal{D}_{\kappa}$ and summation of the results yield

$$\begin{split} \overline{\langle \boldsymbol{v}^{\kappa}, \boldsymbol{\tau} \rangle}_{\partial \mathcal{B}_{t}} = & \langle \left((\rho_{\kappa} - \rho)\omega^{2}\boldsymbol{u}^{\tau} \big|_{\mathcal{D}_{\kappa}^{\star} \backslash \overline{\Gamma_{\kappa}}'}, -(\overline{C_{\kappa}} - C) : \nabla \boldsymbol{u}^{\tau} \big|_{\mathcal{D}_{\kappa}^{\star} \backslash \overline{\Gamma_{\kappa}}'}, \left[\boldsymbol{u}^{\tau} \right] \right|_{\Gamma_{\kappa}}, \boldsymbol{u}^{\tau} \big|_{\partial \mathcal{D}_{\kappa}^{o}}), \\ & \left(\boldsymbol{u}^{f} \big|_{\mathcal{D}_{\kappa}^{\star} \backslash \overline{\Gamma_{\kappa}}'}, \nabla \boldsymbol{u}^{f} \big|_{\mathcal{D}_{\kappa}^{\star} \backslash \overline{\Gamma_{\kappa}}'}, t[\boldsymbol{u}^{f}] \big|_{\Gamma_{\kappa}}, t[\boldsymbol{u}^{f}] \big|_{\partial \mathcal{D}_{\kappa}^{o}} \right) \right)_{\mathcal{D}_{\kappa}^{\star} \cup \Gamma_{\kappa} \cup \partial \mathcal{D}_{\kappa}^{o}'} \end{split}$$

substantiating (4.11) as the adjoint operator. Next, let $\tau \in L^2(\partial \mathcal{B}_t)^3$ and assume that $\mathcal{V}_{\kappa}^*(\tau) = \mathbf{0}$, i.e.

$$\left(u^{\tau}\big|_{\mathcal{D}_{\kappa}^{\star}\setminus\overline{\Gamma_{\kappa}}'},\nabla u^{\tau}\big|_{\mathcal{D}_{\kappa}^{\star}\setminus\overline{\Gamma_{\kappa}}'},\llbracket u^{\tau}\rrbracket\big|_{\Gamma_{\kappa}},u^{\tau}\big|_{\partial\mathcal{D}_{\kappa}^{o}}\right)=0.$$

In this setting, the unique continuation reads $u^{\tau} = 0$, and thus, $\tau = 0$ which concludes the proof.

Assumption 4.8. Under assumptions 2.2 and 2.3, one of the following applies:

— $\Re(C_{\kappa} - C) - \alpha \Im(C_{\kappa})$ is positive definite on $\mathcal{D}_{\kappa}^{\star} \setminus \overline{\Gamma_{\kappa}}$ for some constant $\alpha \ge 0$. — For some constants $\alpha, \eta > 0$,

$$\overline{\mathbf{X}}: \Re(C-C_{\kappa}): \mathbf{X} \geq \alpha |\mathbf{X}|^2, \quad \overline{\mathbf{X}}: \Re(C_{\kappa}): \mathbf{X} \geq \eta |\mathbf{X}|^2, \quad \|\Im(C_{\kappa})\|_{L^{\infty}} < \sqrt{\alpha \eta},$$
 on $\mathcal{D}_{\kappa}^{\star} \setminus \overline{\varGamma_{\kappa}}$ for all \mathbf{X} in $\mathbb{C}^{3 \times 3}$.

Lemma 4.9. Under assumptions 2.1, 2.2, 2.3, 4.5 and 4.8, the operator $T_{\kappa}:\mathfrak{S}(H_{\Delta})\to \tilde{S}(\mathcal{D}_{\kappa}^{\star}\cup \Gamma_{\kappa}\cup \mathcal{D}_{\kappa})$ $\partial \mathcal{D}^{0}_{\kappa}$) is coercive, i.e. there exists a constant c>0 independent of Ξ such that

$$|\langle T_{\kappa} \Xi, \Xi \rangle| \ge c \parallel \Xi \parallel_{S(\mathcal{D}_{\kappa}^{*} \cup \Gamma_{\kappa} \cup \partial \mathcal{D}_{v}^{0})}^{2}, \quad \forall \Xi \in \mathfrak{S}(H_{\Delta}). \tag{4.12}$$

Proof. We adopt a contradiction argument as follows. Suppose (4.12) does not hold, then one may find a sequence $(\Xi_n)_{n\in\mathbb{N}}\subset\mathfrak{S}(H_\Delta)$ such that

$$\| \boldsymbol{\Xi}_n \|_{S(\mathcal{D}_{\kappa}^{\star} \cup \Gamma_{\kappa} \cup \partial \mathcal{D}_{\kappa}^0)} = 1, \quad |\langle T_{\kappa} \boldsymbol{\Xi}_n, \boldsymbol{\Xi}_n \rangle| \to 0 \text{ as } n \to \infty.$$
 (4.13)

Denote by $v^n \in H^1(\mathcal{B}_{\kappa}^- \cup \mathcal{D}_{\kappa}^{\star} \setminus \overline{\Gamma_{\kappa}})^3$ the solution to (2.5) with

$$(u^{\mathbf{f}}|_{\mathcal{D}_{\kappa}^{*}\backslash\overline{\Gamma_{\kappa}}}, \nabla u^{\mathbf{f}}|_{\mathcal{D}_{\kappa}^{*}\backslash\overline{\Gamma_{\kappa}}}, t[u^{\mathbf{f}}]|_{\Gamma_{\kappa}}, t[u^{\mathbf{f}}]|_{\partial\mathcal{D}_{\kappa}^{0}}) = \Xi_{n}$$

$$:= (u^{n}|_{\mathcal{D}_{\kappa}^{*}\backslash\overline{\Gamma_{\kappa}}}, \nabla u^{n}|_{\mathcal{D}_{\kappa}^{*}\backslash\overline{\Gamma_{\kappa}}}, t[u^{n}]|_{\Gamma_{\kappa}\cap\overline{\mathcal{D}_{\kappa}^{*}}} \oplus \psi^{n}, \phi^{n}),$$

$$\nabla \cdot C : \nabla u^{n} + \rho \omega^{2} u^{n} = \mathbf{0} \text{ in } \mathcal{D}_{\kappa}^{*}, \quad (\psi^{n}, \phi^{n}) \in H^{-1/2}(\Gamma_{\kappa} \setminus \overline{\mathcal{D}_{\kappa}^{*}})^{3} \times H^{-1/2}(\partial\mathcal{D}_{\kappa}^{0})^{3}.$$

Elliptic regularity implies that $\|v^n\|_{H^2(\mathcal{B}_{\nu}^{-})^3}$ is bounded uniformly with respect to n. Then, up to changing the initial sequence, one may assume that Ξ_n weakly converges to some Ξ in $S(\mathcal{D}_{\kappa}^{\star} \cup \Gamma_{\kappa} \cup \partial \mathcal{D}_{\kappa}^{0})$ and v^{n} converges weakly in $H^{2}(\mathcal{B}_{\kappa}^{-})^{3} \cap H^{1}(\mathcal{D}_{\kappa}^{\star} \setminus \overline{\Gamma_{\kappa}})^{3}$ to some $v \in H^{2}(\mathcal{B}_{\kappa}^{-})^{3} \cap H^{2}(\mathcal{B}_{\kappa}^{-})^{3}$ $H^1(\mathcal{D}_{\kappa}^{\star} \setminus \overline{\mathcal{I}_{\kappa}})^3$. Now, observe that \boldsymbol{v} satisfies (2.5) for

$$\boldsymbol{\Xi} = (\boldsymbol{u}|_{\mathcal{D}_{\kappa}^{\star} \setminus \overline{\Gamma_{\kappa}}}, \nabla \boldsymbol{u}|_{\mathcal{D}_{\kappa}^{\star} \setminus \overline{\Gamma_{\kappa}}}, \boldsymbol{t}[\boldsymbol{u}]|_{\Gamma_{\kappa} \cap \overline{\mathcal{D}_{\kappa}^{\star}}} \oplus \boldsymbol{\psi}, \boldsymbol{\phi}), \quad (\boldsymbol{\psi}, \boldsymbol{\phi}) \in H^{-1/2}(\Gamma_{\kappa} \setminus \overline{\mathcal{D}_{\kappa}^{\star}})^{3} \times H^{-1/2}(\partial \mathcal{D}_{\kappa}^{0})^{3},$$

wherein $\nabla \cdot C : \nabla u + \rho \omega^2 u = 0$ in $\mathcal{D}_{\kappa}^{\star}$. In this setting, (4.9) along with $|\langle T_{\kappa} \Xi_n, \Xi_n \rangle| \to 0$ imply that $\llbracket v^n \rrbracket \to \mathbf{0}$ on Γ_{κ} and $\nabla (u^n + v^n) \to \mathbf{0}$ in $\mathcal{D}_{\kappa}^{\star} \setminus \overline{\Gamma_{\kappa}}$, whereby the first of (2.5) reads that $u^n + v^n \to \mathbf{0}$ in $\mathcal{D}_{\kappa}^{*}\setminus\overline{\Gamma_{\kappa}}$. One may then deduce from the unique continuation principle that the total field $u^{n}+v^{n}$ also vanishes in \mathcal{B}_{κ}^- . In which case, (2.9) indicates that $v^n \to 0$, and thus v = 0, on $\partial \mathcal{B}_t$. This implies that (a) $\psi = \phi = 0$ by virtue of the second and fifth of (2.5) and the unique continuation, and (b) u = v = 0 which follows from assumption 4.5.

Next, on recalling (3.6) and (3.7), (4.13) may be recast as

$$\langle T_{\kappa} \boldsymbol{\Xi}_{n}, \boldsymbol{\Xi}_{n} \rangle = -\int_{\mathcal{D}_{\kappa}^{*} \backslash \overline{\Gamma_{\kappa}}} \left[\nabla \bar{\boldsymbol{u}}^{n} : (\boldsymbol{C}_{\kappa} - \boldsymbol{C}) : \nabla (\boldsymbol{u}^{n} + \boldsymbol{v}^{n}) + \omega^{2} (\rho - \rho_{\kappa}) \bar{\boldsymbol{u}}^{n} \cdot (\boldsymbol{u}^{n} + \boldsymbol{v}^{n}) \right] dV$$

$$+ \int_{\Gamma_{\kappa} \cap \overline{\mathcal{D}_{\kappa}^{*}}} \bar{\boldsymbol{t}} [\boldsymbol{u}^{n}] \cdot [\![\boldsymbol{v}^{n}]\!] dS + \int_{\Gamma_{\kappa} \backslash \overline{\mathcal{D}_{\kappa}^{*}}} \bar{\boldsymbol{\psi}}^{n} \cdot [\![\boldsymbol{v}^{n}]\!] dS + \int_{\partial \mathcal{D}_{\kappa}^{o}} \bar{\boldsymbol{\phi}}^{n} \cdot (\boldsymbol{u}_{\phi}^{n} + \boldsymbol{v}^{n}) dS, \tag{4.14}$$

where u_{ϕ}^{n} solves

$$\begin{cases}
\nabla \cdot C : \nabla u_{\phi}^{n}(\xi) + \rho \omega^{2} u_{\phi}^{n}(\xi) = \mathbf{0}, & \xi \in \mathcal{D}_{\kappa}^{0}, \\
n \cdot C : \nabla u_{\phi}^{n}(\xi) = \phi^{n}(\xi), & \xi \in \partial \mathcal{D}_{\kappa}^{0}.
\end{cases}$$
(4.15)

In addition, the variational form (A 1) with $v^{\kappa} = v' = v^n$ reads

$$\int_{\mathcal{D}_{\kappa}^{\bullet} \setminus \overline{\Gamma_{\kappa}}} \left[\nabla \bar{\boldsymbol{v}}^{n} : (C_{\kappa} - C) : \nabla (\boldsymbol{u}^{n} + \boldsymbol{v}^{n}) + \omega^{2} (\rho - \rho_{\kappa}) \bar{\boldsymbol{v}}^{n} \cdot (\boldsymbol{u}^{n} + \boldsymbol{v}^{n}) \right] dV
- \int_{\Gamma_{\kappa} \cap \overline{\mathcal{D}_{\kappa}^{\bullet}}} \boldsymbol{t} [\boldsymbol{u}^{n}] \cdot [\![\bar{\boldsymbol{v}}^{n}]\!] dS - \int_{\Gamma_{\kappa} \setminus \overline{\mathcal{D}_{\kappa}^{\bullet}}} \boldsymbol{\psi}^{n} \cdot [\![\bar{\boldsymbol{v}}^{n}]\!] dS - \int_{\partial \mathcal{D}_{\kappa}^{0}} \boldsymbol{\phi}^{n} \cdot \bar{\boldsymbol{v}}^{n} dS
= - \int_{\mathcal{B}_{\kappa}^{-} \cup \mathcal{D}_{\kappa}^{\bullet} \setminus \overline{\Gamma_{\kappa}}} \left[\nabla \bar{\boldsymbol{v}}^{n} : C : \nabla \boldsymbol{v}^{n} - \rho \omega^{2} \bar{\boldsymbol{v}}^{n} \cdot \boldsymbol{v}^{n} \right] dV - \int_{\Gamma_{\kappa}} [\![\bar{\boldsymbol{v}}^{n}]\!] \cdot K_{\kappa} [\![\boldsymbol{v}^{n}]\!] dS.$$
(4.16)

Since $|\langle T_K \Xi_n, \Xi_n \rangle| \to 0$ as $n \to \infty$, (4.14) in light of the Rellich compact embedding theorem along with the regularity of the trace operator implies that

$$\int_{\mathcal{D}^{\bullet} \setminus \overline{C_{\kappa}}} \nabla \bar{\boldsymbol{u}}^{n} : (C_{\kappa} - C) : \nabla (\boldsymbol{u}^{n} + \boldsymbol{v}^{n}) \, dV \to 0 \quad \text{as } n \to \infty.$$

$$(4.17)$$

Similarly, the compact embedding and trace theorems applied to (4.16) read

$$\int_{\mathcal{D}_{\kappa}^{\star}\setminus\overline{\Gamma_{\kappa}}} \nabla \bar{\boldsymbol{v}}^{n} : (\boldsymbol{C}_{\kappa} - \boldsymbol{C}) : \nabla(\boldsymbol{u}^{n} + \boldsymbol{v}^{n}) \, dV + \int_{\mathcal{B}_{\kappa}^{-}\cup\mathcal{D}_{\kappa}^{\star}\setminus\overline{\Gamma_{\kappa}}} \nabla \bar{\boldsymbol{v}}^{n} : \boldsymbol{C} : \nabla \boldsymbol{v}^{n} \, dV \to 0, \tag{4.18}$$

as $n \to \infty$. On superimposing (4.17) and (4.18), one finds

$$\int_{\mathcal{D}_{\kappa}^{+} \setminus \overline{\Gamma_{\kappa}}} \nabla(\bar{\boldsymbol{u}}^{n} + \bar{\boldsymbol{v}}^{n}) : (\boldsymbol{C}_{\kappa} - \boldsymbol{C}) : \nabla(\boldsymbol{u}^{n} + \boldsymbol{v}^{n}) \, d\boldsymbol{V} + \int_{\mathcal{B}_{\kappa}^{-} \cup \mathcal{D}_{\kappa}^{+} \setminus \overline{\Gamma_{\kappa}}} \nabla \bar{\boldsymbol{v}}^{n} : \boldsymbol{C} : \nabla \boldsymbol{v}^{n} \, d\boldsymbol{V} \to 0$$

as $n \to \infty$. Now, following the first of assumption 4.8, where $\Re(C_{\kappa} - C) - \alpha \Im(C_{\kappa})$ is positive definite on $\mathcal{D}_{\kappa}^{\star} \setminus \overline{\Gamma_{\kappa}}$ for some constant $\alpha \ge 0$, observe that

$$\left| \int_{\mathcal{D}_{\kappa}^{*} \setminus \overline{\Gamma_{\kappa}}} \nabla(\bar{\boldsymbol{u}}^{n} + \bar{\boldsymbol{v}}^{n}) : (\boldsymbol{C}_{\kappa} - \boldsymbol{C}) : \nabla(\boldsymbol{u}^{n} + \boldsymbol{v}^{n}) \, d\boldsymbol{V} + \int_{\mathcal{B}_{\kappa}^{-} \cup \mathcal{D}_{\kappa}^{*} \setminus \overline{\Gamma_{\kappa}}} \nabla \bar{\boldsymbol{v}}^{n} : \boldsymbol{C} : \nabla \boldsymbol{v}^{n} \, d\boldsymbol{V} \right|$$

$$\geq \theta \left(\int_{\mathcal{D}_{\kappa}^{*} \setminus \overline{\Gamma_{\kappa}}} \left| \nabla(\boldsymbol{u}^{n} + \boldsymbol{v}^{n}) \right|^{2} \, d\boldsymbol{V} + \int_{\mathcal{B}_{\kappa}^{-} \cup \mathcal{D}_{\kappa}^{*} \setminus \overline{\Gamma_{\kappa}}} \left| \nabla \boldsymbol{v}^{n} \right|^{2} \, d\boldsymbol{V} \right)$$

$$(4.19)$$

for some $\theta > 0$ independent of n. This implies that $\mathbf{v}^n \to \mathbf{0}$ strongly in $H^1(\mathcal{B}_{\kappa}^- \cup \mathcal{D}_{\kappa}^* \setminus \overline{\varGamma_{\kappa}})^3$ which is a contradiction. Given (4.17) and (4.18), the argument for establishing (4.12) for the second case of assumption 4.8 directly follows the proof of theorem 2.42 in [32].

Lemma 4.10. Under assumptions 4.5 and 4.8, the real part of operator $T_{\kappa}:\mathfrak{S}(H_{\Delta})\to \tilde{S}(\mathcal{D}_{\kappa}^{\star}\cup \Gamma_{\kappa}\cup \partial\mathcal{D}_{\kappa}^{0})$ may be decomposed on $\mathfrak{S}(H_{\Delta})$ into a coercive part T_{c}^{\pm} and a compact part T_{c} .

Lemma 4.11. The scattering operator $\Lambda_{\kappa}: L^2(\partial \mathcal{B}_t)^3 \to L^2(\partial \mathcal{B}_t)^3$ is injective, compact and has a dense range.

Proof. The injectivity (*resp.* compactness) of $\Lambda_{\kappa} = \mathcal{V}_{\kappa} \, \mathcal{S}_{\kappa}$ results from the injectivity (*resp.* compactness) of \mathcal{V}_{κ} and \mathcal{S}_{κ} as per lemmas 4.9 and 4.3. Now, according to lemmas 4.4 and 4.9, the adjoint operators \mathcal{S}_{κ}^* , \mathcal{V}_{κ}^* and thus $\Lambda_{\kappa}^* = \mathcal{S}_{\kappa}^* \, \mathcal{V}_{\kappa}^*$ are injective which establish the denseness of the range of Λ_{κ} .

5. Design of imaging functionals

Let us generate a set of sampling points $x_o \in \mathcal{B}$ in the baseline model designating the loci of (monopole and dipole) trial scatterers. Monopole signatures are created via point sources applied along a set of trial directions n, while dipole patterns are constructed by nucleating dislocations $L := x_o + \mathbf{R} \mathbf{L} \subset \mathcal{B}$ in the baseline model wherein \mathbf{L} is a smooth arbitrary-shaped discontinuity whose orientation is given by the unitary rotation matrix $\mathbf{R} \in U(3)$. In this setting, the scattering pattern $\Psi^o : \check{H}^{1/2}(L)^3 \to L^2(\partial \mathcal{B}_t)^3$ is defined by

$$\Psi^{o}(\xi) := (1 - o)n \cdot G(\xi, x_{o}) + o \int_{L} a(y) \cdot T(\xi, y) \, dS_{y}, \quad o \in \{0, 1\}, \ \xi \in \partial \mathcal{B}_{t}, \tag{5.1}$$

for any admissible density $a \in \tilde{H}^{1/2}(L)^3$. Keep in mind that Green's dyadic G satisfies (2.10) and its affiliated traction T on L is specified in (2.9).

To construct a sampling-based imaging functional, we deploy Ψ^0 to explore the range of Λ_{κ} by minimizing the below sequence of cost functions

$$\mathfrak{J}^{\gamma}_{\kappa}(\boldsymbol{\Psi}^{o};\boldsymbol{\tau}) := \|\boldsymbol{\Lambda}_{\kappa}\,\boldsymbol{\tau} - \boldsymbol{\Psi}^{o}\|_{L^{2}(\partial\mathcal{B}_{t})}^{2} + \gamma\left(\boldsymbol{\tau},\boldsymbol{\Lambda}_{\kappa_{\sharp}}\boldsymbol{\tau}\right)_{L^{2}(\partial\mathcal{B}_{t})}, \,\, \boldsymbol{\tau} \in L^{2}(\partial\mathcal{B}_{t})^{3}, \,\, \gamma > 0, \tag{5.2}$$

where $\Lambda_{\kappa_{\sharp}}: L^2(\partial \mathcal{B}_t)^3 \to L^2(\partial \mathcal{B}_t)^3$ is given by

$$\Lambda_{\kappa_{\sharp}} := \frac{1}{2} |\Lambda_{\kappa} + \Lambda_{\kappa}^*| + \frac{1}{2i} (\Lambda_{\kappa} - \Lambda_{\kappa}^*). \tag{5.3}$$

Remark 5.1. Lemmas 4.4, 4.6, 4.7, 4.10 establish the premises of ([59], theorem 2.15) which concludes that operator $\Lambda_{\kappa_{\sharp}}$ is positive and has the following factorization

$$\Lambda_{\kappa_{\sharp}} = \mathcal{S}_{\kappa}^* T_{\kappa_{\sharp}} \, \mathcal{S}_{\kappa}, \tag{5.4}$$

where the middle operator $T_{\kappa_{\sharp}}$ is self-adjoint and positively coercive, i.e. there exists a constant c > 0 independent of Ξ so that

$$\langle T_{\kappa_{\sharp}} \Xi, \Xi \rangle \ge c \parallel \Xi \parallel_{S(\mathcal{D}_{c}^{*} \cup \Gamma_{c} \cup \partial \mathcal{D}_{c}^{0})}^{2}, \forall \Xi \in \mathfrak{S}(H_{\Delta}).$$

$$(5.5)$$

Moreover, the range of S_{κ}^* coincides with that of $\Lambda_{\kappa_{\sharp}}^{1/2}$.

Assumptions and lemmas of §B furnish all the necessary conditions for the fundamental theorems of GLSM [37,40] to apply. These results are required for the differential imaging indicators which for future reference are included in the following.

Theorem 5.2 ([37,40]). Consider the minimizing sequence $\tau^{\gamma} \in L^2(\partial \mathcal{B}_t)^3$ for $\mathfrak{J}_{\kappa}^{\gamma}$ such that

$$\mathfrak{J}_{\kappa}^{\gamma}(\boldsymbol{\Psi}^{o};\boldsymbol{\tau}^{\gamma}) \leq \mathfrak{j}_{\kappa}^{\gamma}(\boldsymbol{\Psi}^{o}) + \eta(\gamma), \quad \gamma > 0, \tag{5.6}$$

where $\eta(\gamma)/\gamma \to 0$ as $\gamma \to 0$ and

$$j_{\kappa}^{\gamma}(\boldsymbol{\Psi}^{o}) := \inf_{\boldsymbol{\tau} \in L^{2}(\partial \mathcal{B}_{t})^{3}} \mathfrak{J}_{\kappa}^{\gamma}(\boldsymbol{\Psi}^{o}; \boldsymbol{\tau}).$$

Then,

$$\begin{cases}
\Psi^{o} \in \mathcal{R}(\mathcal{V}_{\kappa}) \Rightarrow \lim_{\gamma \to 0} (\boldsymbol{\tau}^{\gamma}, \Lambda_{\kappa_{\sharp}} \boldsymbol{\tau}^{\gamma}) < \infty, \\
\Psi^{o} \notin \mathcal{R}(\mathcal{V}_{\kappa}) \Rightarrow \lim_{\gamma \to 0} \inf (\boldsymbol{\tau}^{\gamma}, \Lambda_{\kappa_{\sharp}} \boldsymbol{\tau}^{\gamma}) = \infty.
\end{cases}$$
(5.7)

Moreover, when $V_{\kappa} \Xi = \Psi^{0}$, the sequence $S_{\kappa} \tau^{\gamma}$ strongly converges to $\Xi \in \mathfrak{S}(H_{\Delta})$ as $\gamma \to 0$.

Corollary 5.3. *Under assumptions 2.4 and 4.5,*

$$\Psi^0 \in \mathcal{R}(\mathcal{V}_{\kappa}) \iff x_0 \in \mathcal{D}_{\kappa} \cup \Gamma_{\kappa}.$$

In addition, if

 $-x_{\circ} \in \mathcal{D}_{\kappa}^{\star}$ then there exists a unique solution $(u_{\kappa}^{\star}, w_{\kappa}^{\star})$ to

$$ITP_{\kappa} := ITP(\mathcal{D}_{\kappa}^{\star}, \Gamma_{\kappa}; \{C, \rho\}, \{C_{\kappa}, \rho_{\kappa}\}, K_{\kappa}; n \cdot C : \nabla \Psi^{0}, \Psi^{0}). \tag{5.8}$$

— $x_{\circ} \in \mathcal{D}^{o}_{\kappa}$ then there exists a unique field \mathbf{u}^{o}_{κ} satisfying

$$\begin{cases}
\nabla \cdot (C : \nabla \mathbf{u}_{\kappa}^{o}) + \rho \, \omega^{2} \mathbf{u}_{\kappa}^{o} = \mathbf{0} & \text{in } \mathcal{D}_{\kappa}^{o}, \\
\mathbf{n} \cdot C : \nabla (\mathbf{u}_{\kappa}^{o} + \mathbf{\Psi}^{o}) = \mathbf{0} & \text{on } \partial \mathcal{D}_{\kappa}^{o}.
\end{cases}$$
(5.9)

— $L \subset \Gamma_{\kappa} \setminus \overline{\mathcal{D}_{\kappa}^{\star}}$ then there exists a unique $\llbracket \mathbf{v}_{\kappa} \rrbracket \in \tilde{H}^{1/2}(\Gamma_{\kappa} \setminus \overline{\mathcal{D}_{\kappa}^{\star}})^3$ such that $\mathcal{S}_{\kappa}^{*} \llbracket \mathbf{v}_{\kappa} \rrbracket = \Psi^1$. In this setting, the affiliated free-field traction $\mathbf{t}[\mathbf{u}_{\kappa}^t]$ may be obtained from the second of (2.5),

$$t[u_{\kappa}^{\mathsf{f}}](\xi) = K_{\kappa}(\xi) \llbracket \mathbf{v}_{\kappa} \rrbracket(\xi) - n \cdot C : \nabla \Psi^{1}(\xi), \quad \xi \in \Gamma_{\kappa} \setminus \overline{\mathcal{D}_{\kappa}^{\star}}. \tag{5.10}$$

Now, let us recall from (2.1) that (a) $\mathcal{E}_{i}^{\star} \subset \mathcal{B}$, $i \in \{1, 2, \ldots\}$, is the support of (volumetric) elastic transformation where by assumption 2.3 $\sup(C_{i} - C_{i-1}) = \sup(\rho_{i} - \rho_{i-1})$, and $\mathcal{D}_{i}^{\star} = \mathcal{E}_{i}^{\star} \cup \mathcal{D}_{i-1}^{\star}$ since $\mathcal{D}_{i-1}^{\star} \subset \mathcal{D}_{i}^{\star}$, (b) \mathcal{E}_{i}^{o} designates the evolution of pore volume which is disjoint from \mathcal{E}_{i}^{\star} since $\overline{\mathcal{D}_{i}^{\star}} \cap \overline{\mathcal{D}_{i}^{\circ}} = \emptyset$, and (c) $\hat{\Gamma}_{i} \cup \tilde{\Gamma}_{i}$ represents the support of (geometric $\hat{\Gamma}_{i}$ and elastic $\tilde{\Gamma}_{i}$) interfacial evolution. On denoting by $\mathcal{D}_{i-1,j'}^{\star}$, $j = 1, 2, \ldots, N_{i-1}$ (resp. $\mathcal{D}_{i,j'}^{\star}$, $j = 1, 2, \ldots, N_{i}$) the simply connected

components of $\mathcal{D}_{i-1}^{\star}$ (resp. \mathcal{D}_{i}^{\star}), one may define the set of stationary inclusions

$$\check{\mathcal{D}}_{i-1}^{\star} = \bigcup_{j \in \iota} \mathcal{D}_{i-1,j}^{\star}, \quad \iota = \left\{ j \mid \exists \varkappa \, \mathcal{D}_{i-1,j}^{\star} = \mathcal{D}_{i,\varkappa}^{\star} \, \wedge \, \overline{\mathcal{D}_{i-1,j}^{\star}} \cap \overline{\mathcal{E}_{i}^{\star} \cup \hat{\Gamma}_{i} \cup \tilde{\Gamma}_{i}} = \emptyset \right\}, \tag{5.11}$$

which remain unchanged between $[t_{i-1} \ t_i]$. By adopting a similar notation, the stationary pores are identified by

$$\check{\mathcal{D}}_{i-1}^{o} = \bigcup_{j \in \iota} \mathcal{D}_{i-1,j}^{o}, \quad \iota = \{j \mid \exists x \ \mathcal{D}_{i-1,j}^{o} = \mathcal{D}_{i,x}^{o}\}.$$
 (5.12)

In this setting, $\tilde{\mathcal{D}}_{i-1}^{\tau} := \mathcal{D}_{i-1}^{\tau} \setminus \overline{\check{\mathcal{D}}_{i-1}^{\tau}}$, $\tau = \{\star, o\}$, signifies the evolved subset of \mathcal{D}_{i-1}^{τ} within the same timeframe. Further, one may introduce

$$\tilde{\mathcal{D}}_{i}^{\tau} = \bigcup_{j \in \tilde{\iota}} \mathcal{D}_{i,j}^{\tau}, \quad \tilde{\iota} = \left\{ j \,|\, \overline{\mathcal{D}_{i,j}^{\tau}} \cap \overline{\tilde{\mathcal{D}}_{i-1}^{\tau}} \neq \emptyset \right\}, \ \tau = \{\star, o\}, \tag{5.13}$$

so that \mathcal{E}_i^{τ} may be decomposed into disjoint subsets $\overline{\tilde{\mathcal{E}}_i^{\tau}} = \overline{\mathcal{E}_i^{\tau}} \cap \overline{\tilde{\mathcal{D}}_i^{\tau}}$ and $\hat{\mathcal{E}}_i^{\tau} = \mathcal{D}_i^{\tau} \setminus \{\check{\mathcal{D}}_{i-1}^{\tau} \cup \tilde{\mathcal{D}}_i^{\tau}\}$. Based on this, let us in addition define

$$\check{\Gamma}_{i-1} = \Gamma_{i-1} \setminus \overline{\tilde{\Gamma}_i \cup \tilde{\mathcal{D}}_i^* \cup \mathcal{E}_i^* \cup \mathcal{E}_i^0}. \tag{5.14}$$

While our objective is to design imaging functionals to reconstruct $\mathcal{E}_i^\star \cup \mathcal{E}_i^o \cup \hat{\Gamma}_i \cup \tilde{\Gamma}_i$ given sequential sensory data at t_{i-1} and t_i , one may observe in what follows that the proposed indicator is capable of recovering either $\tilde{\mathcal{D}}_{i-1}^o \cup \tilde{\mathcal{D}}_{i-1}^\star \cup \tilde{\Gamma}_i$ or $\mathcal{E}_i^* \cup \mathcal{E}_i^o \cup \hat{\Gamma}_i \cup \tilde{\Gamma}_i \cup \tilde{\mathcal{D}}_{i-1}^\star \cup \tilde{\mathcal{D}}_{i-1}^o$.

Assumption 5.4. Let us define $(\tilde{C}, \tilde{\rho})$ in \tilde{D}_i^* by

Downloaded from https://royalsocietypublishing.org/ on 04 June 2023

$$(\tilde{C}, \tilde{\rho})(\xi) := \begin{cases} (C_{i-1}, \rho_{i-1})(\xi), & \xi \in \tilde{\mathcal{D}}_{i-1}^{\star} \\ (C, \rho), & \xi \in \tilde{\mathcal{D}}_{i}^{\star} \backslash \tilde{\mathcal{D}}_{i-1}^{\star} \end{cases}$$
(5.15)

then $\omega > 0$ is not a transmission eigenvalue solving

$$\begin{split} & \text{ITP}_{\circ}^{f}(\tilde{\mathcal{E}}_{i}^{\star}, \Gamma_{i-1}, \Gamma_{i}; \{\tilde{C}, \tilde{\rho}\}, \{C_{i}, \rho_{i}\}, K_{i-1}, K_{i}) \\ & = \begin{cases} \nabla \cdot [C_{i}(\xi) : \nabla w_{i}^{\star}](\xi) + \rho_{i}(\xi) \omega^{2} w_{i}^{\star}(\xi) = \mathbf{0}, & \xi \in \tilde{\mathcal{E}}_{i}^{\star} \backslash \overline{\Gamma_{i}}, \\ \nabla \cdot [\tilde{C}(\xi) : \nabla \tilde{w}_{i}^{\star}](\xi) + \tilde{\rho}(\xi) \omega^{2} \tilde{w}_{i}^{\star}(\xi) = \mathbf{0}, & \xi \in \tilde{\mathcal{E}}_{i}^{\star} \backslash \overline{\Gamma_{i-1}}, \\ t[w_{i}^{\star}](\xi) - t[\tilde{w}_{i}^{\star}](\xi) = \mathbf{0}, & [w_{i}^{\star} - \tilde{w}_{i}^{\star}](\xi) = \mathbf{0}, & \xi \in \tilde{\mathcal{E}}_{i}^{\star} \backslash \overline{\Gamma_{i-1}}, \\ t[w_{i}^{\star}](\xi) = K_{i}(\xi) [[w_{i}^{\star}](\xi), [[t[w_{i}^{\star}]]](\xi) = \mathbf{0}, & \xi \in \Gamma_{i} \cap \tilde{\mathcal{E}}_{i}^{\star}, \\ t[w_{i}^{\star}](\xi) = K_{i-1}(\xi) [[\tilde{w}_{i}^{\star}]](\xi), [[t[\tilde{w}_{i}^{\star}]]](\xi) = \mathbf{0}, & \xi \in \Gamma_{i-1} \cap \tilde{\mathcal{E}}_{i}^{\star}, \\ t[w_{i}^{\star}](\xi) - t[\tilde{w}_{i}^{\star}](\xi) = \mathbf{0}, & t[w_{i}^{\star}](\xi), [\tilde{w}_{i}^{\star} - w_{i}^{\star}](\xi), & \xi \in \partial \tilde{\mathcal{E}}_{i}^{\star} \cap \hat{\Gamma}_{i}, \\ t[w_{i}^{\star}](\xi) - t[\tilde{w}_{i}^{\star}](\xi) = \mathbf{0}, & \xi \in [\tilde{w}_{i}^{\star}](\xi), & \xi \in \partial \tilde{\mathcal{E}}_{i}^{\star} \cap \hat{\Gamma}_{i}, \end{cases} \end{split}$$

$$(5.16)$$

Note that special cases such as elastic transformation or growth of intact inclusions are also included in (5.16) and may be obtained by setting $\Gamma_{i-1} = \emptyset$ and/or $\tilde{\Gamma}_i = \hat{\Gamma}_i = \emptyset$ in (5.16). Further, in the case of $\Gamma_{i-1} \cap \hat{\mathcal{E}}_i^{\star} \neq \emptyset$, pertinent to the transformation of microcracked zones, it is assumed that $\omega > 0$ does not satisfy $\operatorname{ITP}_0^{\mathsf{c}}(\hat{\mathcal{E}}_i^{\star}, \Gamma_{i-1}, \Gamma_i; \{C, \rho\}, \{C_i, \rho_i\}, K_{i-1}, K_i)$.

Theorem 5.5. Given assumptions 2.4, 4.1, 4.5, 4.8 and 5.4,

— Let $x_o \in \mathcal{D}_{i-1}^{\star}$ (or $L \subset \mathcal{D}_{i-1}^{\star}$), then denote by $t[u_s^o]$ (resp. $t[u_s^f]$) the free-field traction on $\partial \mathcal{D}_s^o$ (resp. Γ_s) affiliated with the scattering pattern Ψ^o (or τ^{γ}), while $(u_s^{\star}, w_s^{\star})$ uniquely solves ITP_s at times

 $t_s, s \in \{i-1, i\}$. In this setting,

$$If \mathbf{x}_{\circ} \in \check{\mathcal{D}}_{i-1}^{\star} \text{ (or } L \subset \check{\mathcal{D}}_{i-1}^{\star} \text{) then}$$

$$(\mathbf{u}_{i}^{\star}|_{\mathcal{D}_{i-1}^{\star} \setminus \overline{\Gamma_{i-1}}}, \nabla \mathbf{u}_{i}^{\star}|_{\mathcal{D}_{i-1}^{\star} \setminus \overline{\Gamma_{i-1}}}, \mathbf{t}[\mathbf{u}_{i}^{f}]|_{\Gamma_{i-1}}, \mathbf{t}[\mathbf{u}_{i}^{o}]|_{\partial \mathcal{D}_{i-1}^{o}})$$

$$= (\mathbf{u}_{i-1}^{\star}|_{\mathcal{D}_{i-1}^{\star} \setminus \overline{\Gamma_{i-1}}}, \nabla \mathbf{u}_{i-1}^{\star}|_{\mathcal{D}_{i-1}^{\star} \setminus \overline{\Gamma_{i-1}}}, \mathbf{t}[\mathbf{u}_{i-1}^{f}]|_{\Gamma_{i-1}}, \mathbf{t}[\mathbf{u}_{i-1}^{o}]|_{\partial \mathcal{D}_{i-1}^{o}}). \tag{5.17}$$

If
$$\mathbf{x}_{\circ} \in \widetilde{\mathcal{D}}_{i-1}^{\star}$$
 (or $L \subset \widetilde{\mathcal{D}}_{i-1}^{\star}$) then
$$(\mathbf{u}_{i}^{\star}|_{\mathcal{D}_{i-1}^{\star} \setminus \overline{\Gamma_{i-1}}}, \nabla \mathbf{u}_{i}^{\star}|_{\mathcal{D}_{i-1}^{\star} \setminus \overline{\Gamma_{i-1}}}, \mathbf{t}[\mathbf{u}_{i}^{\mathsf{f}}]|_{\Gamma_{i-1} \cap \overline{\mathcal{D}}_{i-1}^{\star}})$$

$$\neq (\mathbf{u}_{i-1}^{\star}|_{\mathcal{D}_{i-1}^{\star} \setminus \overline{\Gamma_{i-1}}}, \nabla \mathbf{u}_{i-1}^{\star}|_{\mathcal{D}_{i-1}^{\star} \setminus \overline{\Gamma_{i-1}}}, \mathbf{t}[\mathbf{u}_{i-1}^{\mathsf{f}}]|_{\Gamma_{i-1} \cap \overline{\mathcal{D}}_{i-1}^{\star}}). \tag{5.18}$$

— Provided that ω is not a Neumann eigenvalue of (5.9) per assumption 4.1, then

If
$$\mathbf{x}_{\circ} \in \check{\mathcal{D}}_{i-1}^{o}$$
 (or $L \subset \check{\mathcal{D}}_{i-1}^{o}$) then (5.17) applies over $\mathcal{D}_{i-1}^{\star} \cup \mathcal{D}_{i-1}^{o} \cup \Gamma_{i-1}$.
If $\mathbf{x}_{\circ} \in \tilde{\mathcal{D}}_{i-1}^{o}$ (or $L \subset \tilde{\mathcal{D}}_{i-1}^{o}$) then
$$\mathbf{t}[\mathbf{u}_{i}^{o}]|_{\partial \mathcal{D}_{i-1}^{o}} \neq \mathbf{t}[\mathbf{u}_{i-1}^{o}]|_{\partial \mathcal{D}_{i-1}^{o}}.$$
(5.19)

- Moreover,

If
$$L \subset \check{\Gamma}_{i-1}$$
 then (5.17) holds.
If $L \subset \Gamma_{i-1} \setminus \overline{\check{\Gamma}_{i-1} \cup \check{\mathcal{D}}_{i-1}^{\star} \cup \check{\mathcal{D}}_{i}^{\star}}$ then
$$t[u_{i}^{t}]|_{\Gamma_{i-1}} \neq t[u_{i-1}^{t}]|_{\Gamma_{i-1}}.$$
(5.20)

Proof. Let $\mathbf{x}_o \in \check{\mathcal{D}}_{i-1}^{\star}$ (resp. $L \subset \check{\mathcal{D}}_{i-1}^{\star}$), then observe that (a) $\mathbf{\Psi}^0$ (resp. $\mathbf{\Psi}^1$) of (5.1) satisfies $\nabla \cdot C$: $\nabla \mathbf{\Psi}^o(\xi) + \rho \, \omega^2 \mathbf{\Psi}^o(\xi) = \mathbf{0}$ in $\boldsymbol{\xi} \in \mathcal{D}_i \setminus \check{\mathcal{D}}_{i-1}^{\star}$ with $o = \{0, 1\}$, and thus, the solution to ITP_s of (5.8) in $\mathcal{D}_s^{\star} \setminus \check{\mathcal{D}}_{i-1}^{\star}$ is given by $(\mathbf{u}_s^{\star}, \mathbf{w}_s^{\star}) = (-\mathbf{\Psi}^o, \mathbf{0})$ for $s = \{i, i-1\}$, (b) $\mathbf{t}[\mathbf{u}_s^o]|_{\partial \mathcal{D}_s^o} = -\mathbf{t}[\mathbf{\Psi}^o]|_{\partial \mathcal{D}_s^o}$ in light of (a) and (5.9), and (c) in corollary 5.3, $[\![\mathbf{v}_s]\!] = \mathbf{0}$ on $\Gamma_s \setminus \check{\mathcal{D}}_{i-1}^{\star}$ which with reference to the contact law per the second of (2.5) implies $\mathbf{t}[\mathbf{u}_s^i]|_{\Gamma_s \setminus \check{\mathcal{D}}_{i-1}^{\star}} = -\mathbf{t}[\mathbf{\Psi}^o]|_{\Gamma_s \setminus \check{\mathcal{D}}_{i-1}^{\star}}$. Further, note from (5.8) and (5.11) that by definition $\mathrm{ITP}_{i-1} = \mathrm{ITP}_i$ in $\check{\mathcal{D}}_{i-1}^{\star}$ so that

$$\begin{split} &(\boldsymbol{u}_{i-1}^{\star}|_{\mathcal{D}_{i-1}^{\star}\setminus\overline{\varGamma_{i-1}}},\nabla\boldsymbol{u}_{i-1}^{\star}|_{\mathcal{D}_{i-1}^{\star}\setminus\overline{\varGamma_{i-1}}},t[\boldsymbol{u}_{i-1}^{f}]|_{\varGamma_{i-1}},t[\boldsymbol{u}_{i-1}^{o}]|_{\partial\mathcal{D}_{i-1}^{o}}))\\ &=(\boldsymbol{u}_{i-1}^{\star}|_{\check{\mathcal{D}}_{i-1}^{\star}\setminus\overline{\varGamma_{i-1}}}\oplus-\boldsymbol{\Psi}^{o}|_{\check{\mathcal{D}}_{i-1}^{\star}},\nabla\boldsymbol{u}_{i-1}^{\star}|_{\check{\mathcal{D}}_{i-1}^{\star}\setminus\overline{\varGamma_{i-1}}}\oplus-\nabla\boldsymbol{\Psi}^{o}|_{\check{\mathcal{D}}_{i-1}^{\star}},\\ &t[\boldsymbol{u}_{i-1}^{\star}]|_{\varGamma_{i-1}\cap\check{\mathcal{D}}_{i-1}^{\star}}\oplus-t[\boldsymbol{\Psi}^{o}]|_{\varGamma_{i-1}\setminus\check{\mathcal{D}}_{i-1}^{\star}},-t[\boldsymbol{\Psi}^{o}]|_{\partial\mathcal{D}_{i-1}^{o}}),\\ &(\boldsymbol{u}_{i}^{\star}|_{\mathcal{D}_{i}^{\star}\setminus\overline{\varGamma_{i}}},\nabla\boldsymbol{u}_{i}^{\star}|_{\mathcal{D}_{i}^{\star}\setminus\overline{\varGamma_{i}}},t[\boldsymbol{u}_{i}^{f}]|_{\varGamma_{i}},t[\boldsymbol{u}_{i}^{o}]|_{\partial\mathcal{D}_{i}^{o}})=(\boldsymbol{u}_{i-1}^{\star}|_{\check{\mathcal{D}}_{i-1}^{\star}\setminus\overline{\varGamma_{i-1}}}\oplus-\boldsymbol{\Psi}^{o}|_{\hat{\mathcal{E}}_{i}^{\star}\cup\tilde{\mathcal{D}}_{i}^{\star}\setminus\overline{\varGamma_{i}}},\\ &\nabla\boldsymbol{u}_{i-1}^{\star}|_{\check{\mathcal{D}}_{i-1}^{\star}\setminus\overline{\varGamma_{i-1}}}\oplus-\nabla\boldsymbol{\Psi}^{o}|_{\hat{\mathcal{E}}_{i}^{\star}\cup\tilde{\mathcal{D}}_{i}^{\star}\setminus\overline{\varGamma_{i}}},t[\boldsymbol{u}_{i-1}^{\star}]|_{\varGamma_{i-1}\cap\check{\mathcal{D}}_{i-1}^{\star}}\oplus-t[\boldsymbol{\Psi}^{o}]|_{\varGamma_{i}\setminus\check{\mathcal{D}}_{i-1}^{\star}},-t[\boldsymbol{\Psi}^{o}]|_{\partial\mathcal{D}_{i}^{o}}), \end{split}$$

establishing (5.17). When $x_{\circ} \in \check{\mathcal{D}}_{i-1}^{o}$ or $L \subset \check{\mathcal{D}}_{i-1}^{o}$, a similar argument leveraging (5.9) leads to

$$\begin{aligned} &(\boldsymbol{u}_{s}^{\star}|_{\mathcal{D}_{s}^{\star}\backslash\overline{\Gamma_{s}}},\nabla\boldsymbol{u}_{s}^{\star}|_{\mathcal{D}_{s}^{\star}\backslash\overline{\Gamma_{s}}},t[\boldsymbol{u}_{s}^{f}]|_{\Gamma_{s}},t[\boldsymbol{u}_{s}^{0}]|_{\partial\mathcal{D}_{s}^{o}}) = (-\boldsymbol{\Psi}^{o}|_{\mathcal{D}_{s}^{\star}\backslash\overline{\Gamma_{s}}},\\ &-\nabla\boldsymbol{\Psi}^{o}|_{\mathcal{D}_{s}^{\star}\backslash\overline{\Gamma_{s}}},-t[\boldsymbol{\Psi}^{o}]|_{\Gamma_{s}},t[\boldsymbol{u}_{i-1}^{o}]|_{\partial\mathcal{\tilde{D}}_{i-1}^{o}} \oplus -t[\boldsymbol{\Psi}^{o}]|_{\partial\mathcal{\tilde{D}}_{i}^{o}\backslash\partial\mathcal{\tilde{D}}_{i-1}^{o}}),s \in \{i-1,i\}, \end{aligned}$$

which confirms (5.17). The same argument as above along with the proof of theorem 4.5 in [40] leads to (5.17) when $L \subset \check{\Gamma}_{i-1}$.

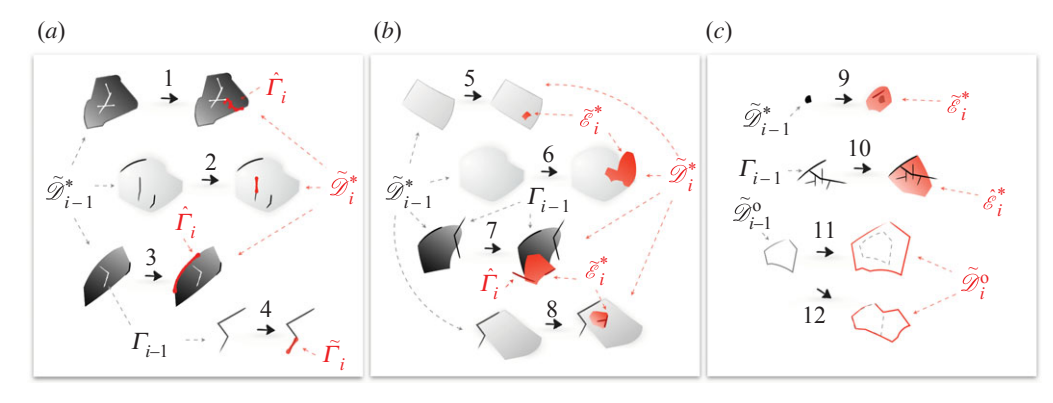


Figure 2. Twelve scenarios for microstructural transformation: (a) geometric expansion and/or elastic modification of discontinuity surfaces in inclusions or the binder, (b) new or modified (fractured) inclusions intersecting with previous (cracked) heterogeneities and (c) newborn inclusions masking the microcracked damage zones and expansion of cavities.

Let $x_0 \in \tilde{\mathcal{D}}_{i-1}^{\star}$ (or $L \subset \tilde{\mathcal{D}}_{i-1}^{\star}$), then in light of the above observe that

$$\begin{split} &(\boldsymbol{u}_{s}^{\star}|_{\mathcal{D}_{s}^{\star}\backslash\overline{\tilde{\mathcal{D}}_{s}^{\star}\cup\Gamma_{s}}},\nabla\boldsymbol{u}_{s}^{\star}|_{\mathcal{D}_{s}^{\star}\backslash\overline{\tilde{\mathcal{D}}_{s}^{\star}\cup\Gamma_{s}}},t[\boldsymbol{u}_{s}^{f}]|_{\Gamma_{s}\backslash\overline{\tilde{\mathcal{D}}_{s}^{\star}}},t[\boldsymbol{u}_{s}^{o}]|_{\partial\mathcal{D}_{s}^{o}})\\ &=(-\boldsymbol{\Psi}^{o}|_{\mathcal{D}_{s}^{\star}\backslash\overline{\tilde{\mathcal{D}}_{s}^{\star}\cup\Gamma_{s}}},-\nabla\boldsymbol{\Psi}^{o}|_{\mathcal{D}_{s}^{\star}\backslash\overline{\tilde{\mathcal{D}}_{s}^{\star}\cup\Gamma_{s}}},-t[\boldsymbol{\Psi}^{o}]|_{\Gamma_{s}\backslash\overline{\tilde{\mathcal{D}}_{s}^{\star}}},-t[\boldsymbol{\Psi}^{o}]|_{\partial\mathcal{D}_{s}^{o}}),\ s\in\{i-1,i\}. \end{split}$$

Next, a contradiction argument is adopted to analyse u_s^* in $\tilde{\mathcal{D}}_s^*$, $s \in \{i-1,i\}$, as the following. Suppose that (5.18) does not hold, i.e.

$$(u_{i}^{\star}|_{\tilde{\mathcal{D}}_{i-1}^{\star}\backslash\overline{\Gamma_{i-1}}}, \nabla u_{i}^{\star}|_{\tilde{\mathcal{D}}_{i-1}^{\star}\backslash\overline{\Gamma_{i-1}}}, t[u_{i}^{f}]|_{\Gamma_{i-1}\cap\overline{\tilde{\mathcal{D}}_{i-1}^{\star}}})$$

$$= (u_{i-1}^{\star}|_{\tilde{\mathcal{D}}_{i-1}^{\star}\backslash\overline{\Gamma_{i-1}}}, \nabla u_{i-1}^{\star}|_{\tilde{\mathcal{D}}_{i-1}^{\star}\backslash\overline{\Gamma_{i-1}}}, t[u_{i-1}^{f}]|_{\Gamma_{i-1}\cap\overline{\tilde{\mathcal{D}}_{i-1}^{\star}}}),$$

$$(5.21)$$

and consider the 12 generic configurations shown in figure 2 for microstructural evolution. The argument for similar or compound scenarios may be drawn from the following case studies. Keep in mind that the ITPs of disconnected sets are independent. Based on this, $\tilde{\mathcal{D}}_{i-1}^{\star}$, in each case, should be understood as the simply connected domain $x_0 \in \mathcal{D}_{i-1,i}^{\star} \subset \tilde{\mathcal{D}}_{i-1}^{\star}$ (or $\mathcal{D}_{i-1,i}^{\star} \supset L$) as defined earlier.

Cases 1–3 (fracturing of inclusions). With reference to figure 2a, consider the case where x_0 (or L) is in $\tilde{\mathcal{D}}_{i-1}^{\star}$ where evolution occurs either by new internal/boundary fractures $\hat{\Gamma}_i$ or by elastically modified interfaces $\tilde{\Gamma}_i$. Under the premise of (5.21), let us define $\mathbf{w} = w_i^* - w_{i-1}^*$ in $\tilde{\mathcal{D}}_{i-1}^* \setminus \overline{\Gamma}_i$. On recalling (4.7), observe that the Cauchy data of \mathbf{w} vanishes on $\partial \tilde{\mathcal{D}}_{i-1}^{\star} \setminus \overline{\Gamma_i}$ which implies by the unique continuation principle that $\mathbf{w} = \mathbf{0}$ in $\tilde{\mathcal{D}}_{i-1}^{\star}$. In case 1—where $\tilde{\mathcal{D}}_{i}^{\star}$ is endowed with internal $\hat{\Gamma}_i$ —the contradiction arises from the discontinuity of w_i^\star across $\hat{\Gamma}_i$ while w_{i-1}^\star is continuous. The only exception to the latter, according to the fourth of (4.7), is when $t[w_i^*] = 0$ on $\hat{\Gamma}_i$ so that $[w_i^*]$ 0, which may not be the case per assumption 4.1. In case 2—where the contact's elasticity K_s with $s \in \{i-1,i\}$ changes over $\tilde{\Gamma}_i$ i.e., $K_{i-1} \neq K_i$ —vanishing **w** in $\tilde{\mathcal{D}}_{i-1}^{\star}$ implies $(K_i - K_{i-1})[[w_i^{\star}]] =$ $(K_i - K_{i-1})[[w_{i-1}^{\star}]] = 0$ on $\tilde{\Gamma}_i$, by the fourth of (4.7), which requires $t[w_i^{\star}] = t[w_{i-1}^{\star}] = 0$ over $\tilde{\Gamma}_i$ that contradicts assumption 4.1. In case 3—where $\hat{\Gamma}_i \subset \partial \hat{\mathcal{D}}_i^*$ —the contradiction may be observed from the fifth of (4.7) where $\mathbf{w} = \mathbf{0}$ reads $t[\mathbf{w}_{i}^{\star}] = \mathbf{0}$ on $\hat{\Gamma}_{i}$ with similar contradiction to assumption 4.1.

Case 4 (evolution of elastic contacts). In this case where $L \subset \tilde{\Gamma}_i \setminus \overline{\mathcal{D}_i^{\star}} \subset \Gamma_{i-1} \setminus \check{\Gamma}_{i-1}$, the fracture stiffness evolves within the matrix, as shown in figure 2a, such that $K_i \neq K_{i-1}$ on $\tilde{\Gamma}_i \setminus \overline{\mathcal{D}_i^{\star}}$. Then, (5.20) is directly concluded from theorem 4.5 and theorem 4.7 of [40]. This may also be observed from (5.10).

Cases 5 and 6 (volumetric growth or transformation of intact inclusions). The premise, as depicted in figure 2b, is that $\overline{\tilde{\mathcal{D}}_{i-1}^{\star}} \cap \Gamma_i = \overline{\tilde{\mathcal{D}}_i^{\star}} \cap \Gamma_i = \emptyset$. In this case, the contradiction to (5.21) may be argued similarly to the proof of theorem 4.2 in [37] which establishes (5.18).

Cases 7–9 (elastic transformation or expansion of fractured inclusions). Let us define \tilde{w}_i^{\star} in $\tilde{\mathcal{D}}_i^{\star}$ as the following:

$$\tilde{w}_{i}^{\star}(\xi) := \begin{cases} w_{i-1}^{\star}(\xi), & \xi \in \tilde{\mathcal{D}}_{i-1}^{\star} \backslash \overline{\Gamma_{i-1}} \\ [u_{i}^{\star} + \Psi^{o}](\xi), & \xi \in \tilde{\mathcal{D}}_{i}^{\star} \backslash \tilde{\mathcal{D}}_{i-1}^{\star} \end{cases},$$
(5.22)

Observe in light of (5.8) and (5.21) that \tilde{w}_i^* solves

$$\nabla \cdot \tilde{\mathbf{C}} : \nabla \tilde{\mathbf{w}}_{i}^{\star} + \tilde{\rho} \,\omega^{2} \tilde{\mathbf{w}}_{i}^{\star} = \mathbf{0} \quad \text{in } \tilde{\mathcal{D}}_{i}^{\star} \setminus \overline{\Gamma_{i-1}},$$

wherein $(\tilde{C}, \tilde{\rho})$ is given by (5.15). In this setting, one may show that the Cauchy data affiliated with $\tilde{\mathbf{w}} = \tilde{w}_i^* - w_i^*$ vanish on $\partial \tilde{\mathcal{D}}_i^* \setminus \Gamma_i$ so that (w_i^*, \tilde{w}_i^*) is the solution to $\mathrm{ITP}_{\circ}^{f}(\tilde{\mathcal{D}}_i^*, \Gamma_{i-1}, \Gamma_i; \{\tilde{C}, \tilde{\rho}\}, \{C_i, \rho_i\}, K_{i-1}, K_i)$. To continue, let us consider two configurations: (cases 7, 8) where $\tilde{\mathcal{D}}_{i-1}^*$ is not included in any simply connected part $\tilde{\mathcal{E}}_{i,j}^*$ of $\tilde{\mathcal{E}}_i^*$, and (case 9) where $\tilde{\mathcal{D}}_{i-1}^* \subset \tilde{\mathcal{E}}_{i,j}^*$. Note that in cases 7, 8, $\partial \tilde{\mathcal{D}}_{i-1}^* \cap \partial \tilde{\mathcal{D}}_i^*$ is of non-zero surface measure, then owing to the equality of Cauchy data associated with \tilde{w}_i^* and w_i^* and the fact that $(C_i, \rho_i) = (\tilde{C}, \tilde{\rho}) = (C_{i-1}, \rho_{i-1})$ on $\partial \tilde{\mathcal{D}}_{i-1}^* \cap \partial \tilde{\mathcal{D}}_i^*$ one may conclude that $\tilde{w}_i^* = w_i^*$ on $\tilde{\mathcal{D}}_{i-1}^* \setminus \tilde{\mathcal{E}}_i^*$. Consequently, $(w_i^*, \tilde{w}_i^*)|_{\tilde{\mathcal{E}}_i^*}$ is the solution to $\mathrm{ITP}_{\circ}^f(\tilde{\mathcal{E}}_i^*, \Gamma_{i-1}, \Gamma_i; \{\tilde{C}, \tilde{\rho}\}, \{C_i, \rho_i\}, K_{i-1}, K_i\}$. The latter according to assumption 5.4 implies that $w_i^* = \tilde{w}_i^* = 0$ in $\tilde{\mathcal{E}}_i^*$ which is a contradiction since u_i^* is smooth by definition while Ψ^o features a singularity at x_\circ . In case 9, one may directly deduce from $\tilde{\mathcal{E}}_i^* \supset \tilde{\mathcal{E}}_{i,j}^* = \tilde{\mathcal{D}}_i^*$ and assumption 5.4 that $w_i^* = 0$ in $\tilde{\mathcal{D}}_i^*$ which leads to the same contradiction.

Case 10 (elastic transformation of microcracked damage zones). With reference to figure 2c, consider the case where L coincides with the binder's fractures at t_{i-1} ($L \subset \Gamma_{i-1}$) within a neighbourhood that undergoes elastic evolution at t_i such that $L \subset \Gamma_{i-1} \cap \hat{\mathcal{E}}_i^{\star}$. Contrary to (5.20), let

$$t[u_i^{\star}]|_{\Gamma_{i-1} \cap \hat{\mathcal{E}}_i^{\star}} = t[u_{i-1}^{\mathsf{f}}]|_{\Gamma_{i-1} \cap \hat{\mathcal{E}}_i^{\star}'}$$

wherein both free fields u_{i-1}^f and u_i^\star satisfy $\nabla \cdot C : \nabla(\cdot) + \rho \omega^2(\cdot) = \mathbf{0}$ in $\hat{\mathcal{E}}_i^\star$. Then observe that the latter also governs $\mathbf{u}^i = u_i^\star - u_{i-1}^f$ such that $t[\mathbf{u}^i] = \mathbf{0}$ on $\Gamma_{i-1} \cap \hat{\mathcal{E}}_i^\star$, implying per assumption 4.1 at t_{i-1} that $u_i^\star = u_{i-1}^f$ in $\hat{\mathcal{E}}_i^\star$. Based on which, one may define $\hat{w}_i^\star = u_i^\star + \Psi^1$ in $\hat{\mathcal{E}}_i^\star$ and similar to cases 7–9 conclude that $(w_i^\star, \hat{w}_i^\star)$ is a solution to $\mathrm{ITP}_\circ^f(\hat{\mathcal{E}}_i^\star, \Gamma_{i-1}, \Gamma_i; \{C, \rho\}, \{C_i, \rho_i\}, K_{i-1}, K_i)$, which by assumption 5.4 reads $\hat{w}_i^\star = \mathbf{0}$ requiring that $u_i^\star = -\Psi^1$ in $\hat{\mathcal{E}}_i^\star$ which is a contradiction since u_i^\star is smooth by definition while Ψ^1 has a discontinuity across L.

Cases 11–12 (expansion of pores). Consider the case shown in figure 2c where x_o (or L) is in $\tilde{\mathcal{D}}_{i-1}^o$ where the evolution of cavities occurs. In contrast to (5.19), let

$$t[u_i^o]|_{\partial \mathcal{D}_{i-1}^o} = t[u_{i-1}^o]|_{\partial \mathcal{D}_{i-1}^o},$$

where $\boldsymbol{u}_{i-1}^{o}, \boldsymbol{u}_{i}^{o}$, and thus $\boldsymbol{u}^{o} = \boldsymbol{u}_{i}^{o} - \boldsymbol{u}_{i-1}^{o}$ satisfy $\nabla \cdot \boldsymbol{C} : \nabla(\cdot) + \rho \, \omega^{2}(\cdot) = \boldsymbol{0}$ in \mathcal{D}_{i-1}^{o} . Note that $\boldsymbol{t}[\boldsymbol{u}^{o}] = \boldsymbol{0}$ on $\partial \mathcal{D}_{i-1}^{o}$ implying per assumption 4.1 that $\boldsymbol{u}_{i}^{o} = \boldsymbol{u}_{i-1}^{o}$ in \mathcal{D}_{i-1}^{o} . Keep in mind that \boldsymbol{u}_{i-1}^{o} (resp. \boldsymbol{u}_{i}^{o}) solves (5.9) in \mathcal{D}_{i-1}^{o} (resp. \mathcal{D}_{i}^{o}). Then, observe that $\boldsymbol{u}_{i}^{o} = -\boldsymbol{\Psi}^{o}$ solves (5.9) within $\mathcal{D}_{i}^{o} \setminus \overline{\mathcal{D}_{i-1}^{o}}$ provided that $\boldsymbol{u}_{i}^{o} = \boldsymbol{u}_{i-1}^{o}$ in \mathcal{D}_{i-1}^{o} . In this setting, the continuity of \boldsymbol{u}_{i}^{o} across $\partial \boldsymbol{u}_{i-1}^{o} \setminus \partial \boldsymbol{u}_{i}^{o}$ along with the unique continuation principle requires that $\boldsymbol{u}_{i}^{o} = -\boldsymbol{\Psi}^{o}$ in \mathcal{D}_{i-1}^{o} which is a contradiction since \boldsymbol{u}_{i}^{o} is smooth according to (5.9) while $\boldsymbol{\Psi}^{o}$ has either a singularity at \boldsymbol{x}_{o} , or a discontinuity across \boldsymbol{L} per (5.1).

Theorem 5.5 furnishes the main results required to (a) identify the invariants of scattering solutions according to theorem 5.6. which is directly obtained by drawing from ([37], theorem 4.3) and ([40], theorem 4.7), and (b) establish the validity of differential evolution indicators in (5.24) following ([37], corollary 1).

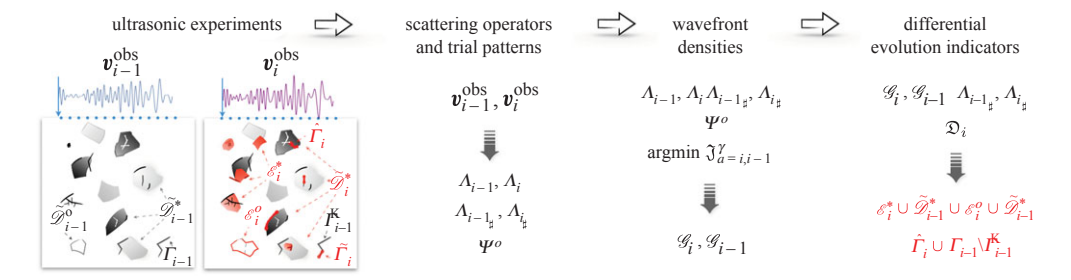


Figure 3. Differential imaging of evolution from sequential waveform data.

Theorem 5.6. Define

$$\chi_i(\mathcal{G}_{i-1}, \mathcal{G}_i) := (\mathcal{G}_i - \mathcal{G}_{i-1}, \Lambda_{i-1}(\mathcal{G}_i - \mathcal{G}_{i-1})), \quad \mathcal{G}_{i-1}, \mathcal{G}_i \in L^2(\Omega)^3,$$
(5.23)

where $(\mathcal{G}_{i-1}, \mathcal{G}_i)(\Psi^o; \gamma)$ are the constructed minimizers of $(\mathfrak{J}_{i-1}^{\gamma}, \mathfrak{J}_{i}^{\gamma})$ in (5.2) according to (5.6). Then, in light of factorization (3.2) and (3.3), theorem 5.5 reads

$$\bullet \ \, If \left| \begin{array}{l} L \subset \check{\mathcal{D}}_{i-1}^{\star} \cup \check{\mathcal{D}}_{i-1}^{o} \cup \check{\Gamma}_{i-1} \\ x_{\circ} \in \check{\mathcal{D}}_{i-1}^{\star} \cup \check{\mathcal{D}}_{i-1}^{o} \end{array} \right. \, , \, \, then \, \, \lim_{\gamma \to 0} \chi_{i}[\mathcal{G}_{i-1}, \mathcal{G}_{i}](\Psi^{o}; \gamma) = 0.$$

$$\begin{split} \bullet \; & If \left| \begin{array}{l} L \subset \check{\mathcal{D}}_{i-1}^{\star} \cup \check{\mathcal{D}}_{i-1}^{o} \cup \check{\Gamma}_{i-1} \\ x_{\circ} \in \check{\mathcal{D}}_{i-1}^{\star} \cup \check{\mathcal{D}}_{i-1}^{o} \end{array} \right. \; , \; then \; \lim_{\gamma \to 0} \chi_{i}[\mathcal{G}_{i-1}, \mathcal{G}_{i}](\boldsymbol{\Psi}^{o}; \gamma) = 0. \\ \bullet \; & If \left| \begin{array}{l} L \subset \tilde{\mathcal{D}}_{i-1}^{\star} \cup \tilde{\mathcal{D}}_{i-1}^{o} \cup \Gamma_{i-1} \setminus \check{\Gamma}_{i-1} \\ x_{\circ} \in \tilde{\mathcal{D}}_{i-1}^{\star} \cup \tilde{\mathcal{D}}_{i-1}^{o} \cup \tilde{\mathcal{D}}_{i-1}^{o} \end{array} \right. \; , \; then \; 0 < \lim_{\gamma \to 0} \chi_{i}[\mathcal{G}_{i-1}, \mathcal{G}_{i}](\boldsymbol{\Psi}^{o}; \gamma) < \infty. \end{split}$$

• If
$$\begin{vmatrix} L \subset \mathcal{E}_{i}^{\star} \setminus \overline{\tilde{\mathcal{D}}_{i-1}^{\star}} \cup \mathcal{E}_{i}^{o} \setminus \overline{\tilde{\mathcal{D}}_{i-1}^{o}} \cup \hat{\mathcal{F}}_{i}^{o} \setminus \overline{\tilde{\mathcal{D}}_{i-1}^{o}} \\ x_{\circ} \in \mathcal{E}_{i}^{\star} \setminus \overline{\tilde{\mathcal{D}}_{i-1}^{\star}} \cup \mathcal{E}_{i}^{o} \setminus \mathcal{\tilde{\mathcal{D}}_{i-1}^{o}} \end{vmatrix} \cup \hat{\Gamma}_{i}^{o} \setminus \overline{\tilde{\mathcal{D}}_{i-1}^{\star}} , \text{ then } \lim_{\gamma \to 0} \chi_{i}[\mathcal{G}_{i-1}, \mathcal{G}_{i}](\boldsymbol{\Psi}^{o}; \gamma) = \infty.$$

(a) Differential evolution indicators

Let us introduce the imaging functionals $\mathfrak{D}_i:L^2(\Omega^3)\times L^2(\Omega^3)\to \mathbb{R}$ and $\tilde{\mathfrak{D}}_i:L^2(\Omega^3)\times L^2(\Omega^3)\to \mathbb{R}$ such that given $\Upsilon_i(\mathcal{G}_i) := (\mathcal{G}_i, \Lambda_{i_{\sharp}} \mathcal{G}_i)$,

$$\begin{cases}
\mathfrak{D}_{i}(\mathcal{G}_{i-1}, \mathcal{G}_{i}) := \frac{1}{\sqrt{\gamma_{i}(\mathcal{G}_{i})[1 + \gamma_{i}(\mathcal{G}_{i})\chi_{i}^{-1}(\mathcal{G}_{i-1}, \mathcal{G}_{i})]}}, \\
\tilde{\mathfrak{D}}_{i}(\mathcal{G}_{i-1}, \mathcal{G}_{i}) := \frac{1}{\sqrt{\gamma_{i-1}(\mathcal{G}_{i-1}) + \gamma_{i}(\mathcal{G}_{i})[1 + \gamma_{i-1}(\mathcal{G}_{i-1})\chi_{i}^{-1}(\mathcal{G}_{i-1}, \mathcal{G}_{i})]}}.
\end{cases} (5.24)$$

Then, it follows that

$$\bullet \begin{vmatrix} L \subset \mathcal{E}_{i}^{\star} \cup \tilde{\mathcal{D}}_{i-1}^{\star} \cup \mathcal{E}_{i}^{o} \cup \tilde{\mathcal{D}}_{i-1}^{o} \cup \hat{\Gamma}_{i} \cup \Gamma_{i-1} \setminus \check{\Gamma}_{i-1} \\ x_{\circ} \in \mathcal{E}_{i}^{\star} \cup \tilde{\mathcal{D}}_{i-1}^{\star} \cup \mathcal{E}_{i}^{o} \cup \tilde{\mathcal{D}}_{i-1}^{o} \end{vmatrix} \iff \lim_{\gamma \to 0} \mathfrak{D}_{i}(\mathcal{G}_{i-1}, \mathcal{G}_{i})(\Psi^{o}; \gamma) > 0$$

and

$$\bullet \begin{vmatrix} L \subset \tilde{\mathcal{D}}_{i-1}^{\star} \cup \tilde{\mathcal{D}}_{i-1}^{o} \cup \Gamma_{i-1} \setminus \check{\Gamma}_{i-1} \\ x_{\circ} \in \tilde{\mathcal{D}}_{i-1}^{\star} \cup \tilde{\mathcal{D}}_{i-1}^{o} \end{vmatrix} \iff \lim_{\gamma \to 0} \tilde{\mathfrak{D}}_{i}(\mathcal{G}_{i-1}, \mathcal{G}_{i})(\Psi^{o}; \gamma) > 0.$$

In other words, \mathfrak{D}_i (resp. $\tilde{\mathfrak{D}}_i$) assumes near-zero values except at the loci of $\mathcal{E}_i^{\star} \cup \tilde{\mathcal{D}}_{i-1}^{\star} \cup \mathcal{E}_i^0 \cup \tilde{\mathcal{D}}_{i-1}^0 \cup \mathcal{D}_{i-1}^0 \cup$ $\hat{\Gamma}_i \cup \Gamma_{i-1} \setminus \check{\Gamma}_{i-1}$ (resp. $\tilde{\mathcal{D}}_{i-1}^{\star} \cup \tilde{\mathcal{D}}_{i-1}^{o} \cup \Gamma_{i-1} \setminus \check{\Gamma}_{i-1}$) where the indicator increases and remains finite as $\gamma \to 0$. By building on ([37], theorem 4.4) and ([40], theorem 4.8), it is quite straightforward to formulate pertinent results for noisy data which for brevity are not included in this paper. To summarize, figure 3 provides the steps for the construction of evolution indicators from numerical or laboratory test data.

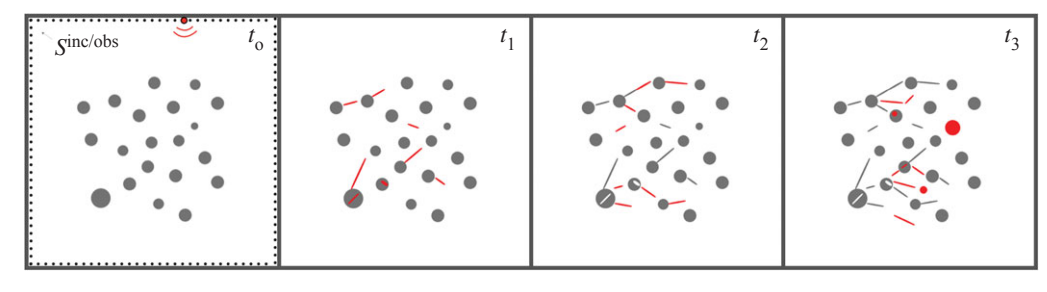


Figure 4. Microstructural geometry of a composite slab with evolving heterogeneities and discontinuities at four sensing steps $t_{\circ} - t_{3}$. Elastic (in-plane) waves are periodically generated via boundary excitations on $S^{\rm inc}$, and the affiliated scattered waveforms are computed over the observation surface $S^{\rm obs}$. Here, $S^{\rm inc} = S^{\rm obs}$ is sampled at 10^{3} points.

6. Synthetic experiments

The evolution indicators of (5.24) are put to the test in this section by a set of numerical experiments. The primary focus is on a randomly heterogeneous and discontinuous background with evolving microstructure due to elastic transformation and/or fracturing. The special cases of *monolithic* solids endowed with crack or pore networks are reported in [40]. In this section, the synthetic scattered fields v_i^{obs} , $i = \{0, 1, 2, 3\}$, are simulated via the boundary element method [60], see [61] for more on the computational platform.

With reference to figure 4, the testing configuration at t_\circ , i.e. the background domain entails a composite slab of dimensions $2.5 \times 2.5 \times 0.01$ comprised of an elastic binder endowed with ellipsoidal inclusions of arbitrary distribution and size. The in-plane diameters of scatterers range from one to five shear wavelengths $\lambda_s = 0.04$, while their pairwise distances are greater than $2\lambda_s$. The normalized shear modulus, mass density and Poisson's ratio of the matrix are taken as $\mu_m = 1$, $\rho_m = 1$ and $\nu_m = 0.25$, while those of the scatterers are $\mu_s = 2$, $\rho_s = \rho_m$ and $\nu_s = \nu_m$. In this setting, the shear and compressional wave speeds in the matrix are $c_m^s = 1$ and $c_m^p = 1.73$. The specimen's microstructural evolution in the following time steps $t_1 - t_3$, according to figure 4, involves (a) multi-step fracturing of the binder and inclusions and their coalescence, (b) elastic transformation of pre-existing inclusions at t_\circ and (c) emergence of new volumetric heterogeneities with shear modulus $\mu_s^{\text{new}} = 1.5$. Note the gradual increase in the evolution complexity, and in particular, the density of scatterers such that at t_3 : (a) the pairwise distance between scatterers may reduce to a small fraction of λ_s , and (b) a subset of evolution support is deeply embedded within the stationary scatterers.

Synthetic experiments are conducted at four time steps $t_{\circ} - t_3$ when the specimen assumes the geometric configurations shown in figure 4. Every sensing step entails 2000 forward simulations where in-plane harmonic waves of frequency $\omega = 140 \text{ rad s}^{-1}$ are generated at a point source over the specimen's external boundary. The resulting scattered fields v_i^{obs} , $i = \{\circ, 1, 2, 3\}$, are then calculated on the same grid by solving the three-dimensional elastodynamics boundary integral equations. Given that λ_s is four times greater than the specimen thickness, the leading contributions to scattered fields are the in-plane components which are then used for data inversion.

The obtained scattered signatures are used to compute the synthetic wavefront densities \mathcal{G}_i , $i = \{\circ, 1, 2, 3\}$, as approximate minimizers of the cost functionals in (5.2). The latter follows the common three steps required for constructing any sampling-based indicator, namely: (i) forming the discrete scattering operators $\Lambda_{i_{\sharp}}$ at every t_i , (ii) assembling the trial signatures Ψ^o of (5.1) as the right-hand side of the scattering equation and (iii) solving the latter by minimizing the discretized cost function (5.2) by invoking the Morozov discrepancy principle. A detailed account of this process is provided in [40]. Given $\Lambda_{i_{\sharp}}$ and \mathcal{G}_i , one may then evaluate the imaging functionals \mathfrak{D}_i from (5.24) which is expected to achieve its highest values at the loci of new and evolved scatterers in each sensing sequence.

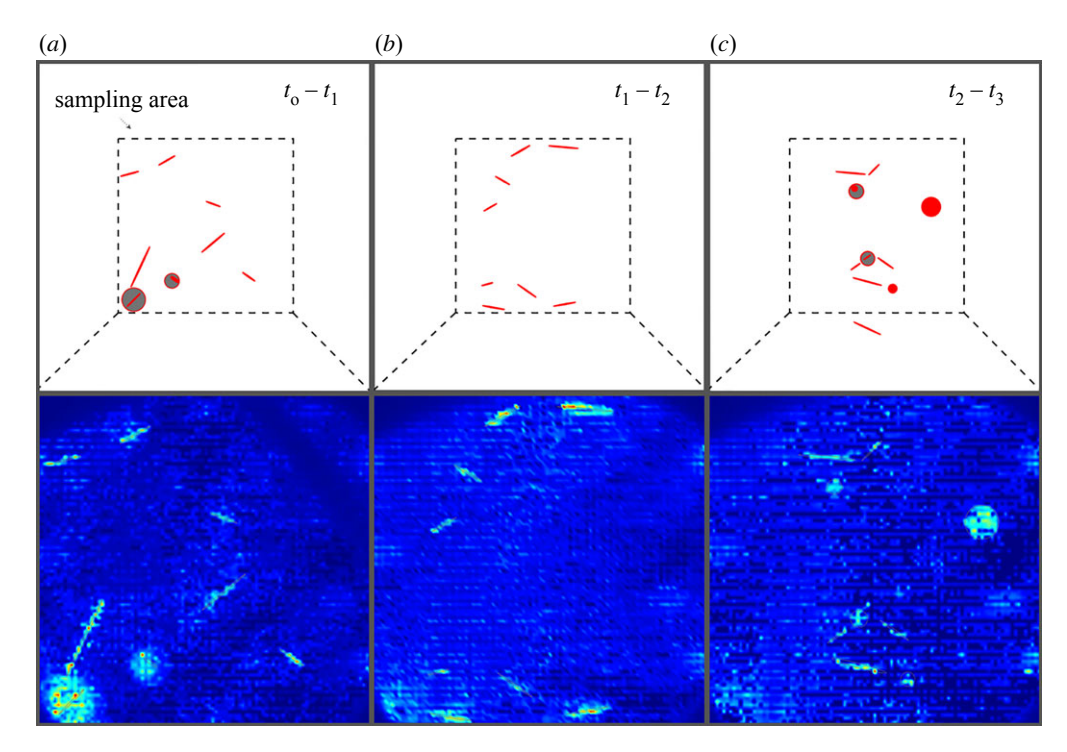


Figure 5. Three-step reconstruction of elastic and interfacial transformations (a-c) of the initial configuration shown in figure 4a: (top) evolution geometry in the sensing sequence $[t_{i-1} t_i]$, $i = \{1, 2, 3\}$, and (bottom) the affiliated indicator map \mathfrak{D}_i of (5.24) computed from the observed scattered field data $\mathbf{v}_{i-1}^{\text{obs}}$ and $\mathbf{v}_i^{\text{obs}}$.

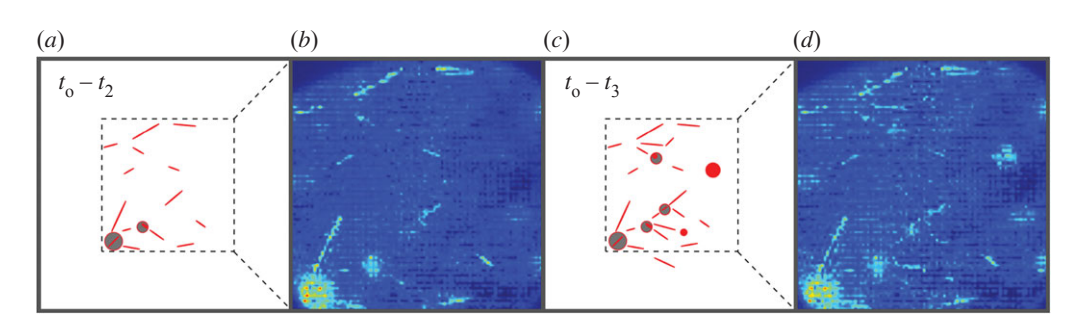


Figure 6. Multi-step reconstruction of elastic and geometric variations: (a,c) true evolution support between $[t_0 \ t_2]$ and $[t_0 \ t_3]$, respectively, and (b,d) the associated (superimposed) differential maps.

Figure 5 illustrates the successive evolution indicators \mathfrak{D}_j , $j=\{1,2,3\}$, over the sampling area. For each time window $t_{j-1}-t_j$, the 'true' support of elastic variations is provided in the top row. Keep in mind that in any sequence, \mathfrak{D}_j is by design insensitive to the scatterers at t_{j-1} provided that they remain unchanged by t_j . The differential maps within $t_\circ-t_2$ feature relatively sharp localizations with minimal artefacts which, given the shear wavelength, may be attributed to the rather sparse distribution of scatterers in this timeframe. Some artefacts emerge in the \mathfrak{D}_3 map, however, since the elastic variations between t_2-t_3 occur within a densely packed network of fractures and inclusions which are assumed to be unknown. To recover the evolution support over an extended timeframe as the microstructure becomes progressively complex, one may superimpose the consecutive reconstructions (of figure 5) as in figure 6.

7. Conclusion

This study furnishes the theoretical foundation for differential evolution indicators for ultrasonic imaging of elastic variations within a heterogeneous and discontinuous background of random structure. In this vein, the well-posedness conditions for the forward and inverse scattering problems are established; in light of which, the pairwise relation between scattering solutions—associated with distinct datasets—is determined. For this purpose, 12 scenarios for microstructural transitions are investigated including (a) fracturing of inclusions, (b) evolution of discontinuity surfaces within each material component or at bimaterial interfaces, (c) elastic transformation and/or expansion of fractured inclusions, (d) conversion of microcracked damage zones and (e) expansion of pores. In all cases, it is shown that certain measures of the synthetic incident fields constructed based on the scattering solutions are, in the limit, equivalent at the loci of unknown scatterers which remain both geometrically and mechanically invariant between a given pair of time steps. This allows for exclusive reconstruction of evolved features without the knowledge (or need for recovery) of stationary components in the background. This is particularly useful in uncertain environments as showcased by the synthetic experiments—provided that the illuminating wavelength is sufficiently smaller than the relevant microstructural length scales, e.g. pairwise distance between the scatterers. Relaxing such constraints may be possible through time-domain inversion as a potential direction in future studies.

Data accessibility. This article has no additional data.

Authors' contributions. F.P.: conceptualization, data curation, formal analysis, funding acquisition, investigation, writing—original draft; H.H.: formal analysis, investigation, writing—review and editing.

All authors gave final approval for publication and agreed to be held accountable for the work performed

Conflict of interest declaration. The authors declare that they have no known competing financial interests or personal relationships that could have appeared to influence the work reported in this paper.

Funding. The corresponding author kindly acknowledges the support provided by the National Science Foundation (grant no. 1944812).

Acknowledgements. This work used resources from the University of Colorado Boulder Research Computing Group, which is supported by the National Science Foundation (awards ACI-1532235 and ACI-1532236), the University of Colorado Boulder and Colorado State University.

Appendix A. Well-posedness of the direct scattering problem

Observe that $\forall v' \in H^1(\mathcal{B}_{\kappa}^- \cup \mathcal{D}_{\kappa}^{\star} \setminus \overline{\Gamma_{\kappa}})^3$, the variational form of (2.5) reads

$$\int_{\mathcal{B}_{\kappa}^{-}} \left[\nabla \, \bar{\boldsymbol{v}}' : \boldsymbol{C} : \nabla \boldsymbol{v}^{\kappa} - \rho \, \omega^{2} \, \bar{\boldsymbol{v}}' \cdot \boldsymbol{v}^{\kappa} \right] dV_{\xi} + \int_{\Gamma_{\kappa}} \left[\boldsymbol{\bar{v}}' \right] \cdot \boldsymbol{K}_{\kappa} \left[\left[\boldsymbol{v}^{\kappa} \right] \right] dS_{\xi}
+ \int_{\mathcal{D}_{\kappa}^{*} \setminus \overline{\Gamma_{\kappa}}} \left[\nabla \, \bar{\boldsymbol{v}}' : \boldsymbol{C}_{\kappa} : \nabla \boldsymbol{v}^{\kappa} - \rho_{\kappa} \omega^{2} \, \bar{\boldsymbol{v}}' \cdot \boldsymbol{v}^{\kappa} \right] dV_{\xi} = \int_{\partial \mathcal{D}_{\kappa}^{0}} \bar{\boldsymbol{v}}' \cdot \boldsymbol{t}^{f} \, dS_{\xi}
+ \int_{\mathcal{D}_{\kappa}^{*} \setminus \overline{\Gamma_{\kappa}}} \left[(\rho_{\kappa} - \rho) \omega^{2} \, \bar{\boldsymbol{v}}' \cdot \boldsymbol{u}^{f} - \nabla \, \bar{\boldsymbol{v}}' : (\boldsymbol{C}_{\kappa} - \boldsymbol{C}) : \nabla \boldsymbol{u}^{f} \right] dV_{\xi} + \int_{\Gamma_{\kappa}} \left[\bar{\boldsymbol{v}}' \right] \cdot \boldsymbol{t}^{f} \, dS_{\xi}. \tag{A 1}$$

The sesquilinear form on the left-hand side of (A 1) may be decomposed as $A(v^{\kappa}, v') + B(v^{\kappa}, v')$ where

$$A(\boldsymbol{v}^{\kappa}, \boldsymbol{v}') = \int_{\mathcal{D}_{\kappa}^{\star} \setminus \overline{\Gamma_{\kappa}}} \left[\nabla \, \bar{\boldsymbol{v}}' : C_{\kappa} : \nabla \boldsymbol{v}^{\kappa} + \, \bar{\boldsymbol{v}}' \cdot \boldsymbol{v}^{\kappa} \right] dV_{\xi} + \int_{\mathcal{B}_{\kappa}^{-}} \left[\nabla \, \bar{\boldsymbol{v}}' : C : \nabla \boldsymbol{v}^{\kappa} + \, \bar{\boldsymbol{v}}' \cdot \boldsymbol{v}^{\kappa} \right] dV_{\xi},$$

$$B(\boldsymbol{v}^{\kappa}, \boldsymbol{v}') = -(1 + \rho_{\kappa} \omega^{2}) \int_{\mathcal{D}_{\kappa}^{\star} \setminus \overline{\Gamma_{\kappa}}} \bar{\boldsymbol{v}}' \cdot \boldsymbol{v}^{\kappa} dV_{\xi} - (1 + \rho\omega^{2}) \int_{\mathcal{B}_{\kappa}^{-}} \bar{\boldsymbol{v}}' \cdot \boldsymbol{v}^{\kappa} dV_{\xi}$$

$$+ \int_{\Gamma_{\kappa}} \left[\left[\bar{\boldsymbol{v}}' \right] \cdot K_{\kappa} \left[\left[\boldsymbol{v}^{\kappa} \right] \right] dS_{\xi}, \quad \forall \boldsymbol{v}' \in H^{1}(\mathcal{B}_{\kappa}^{-} \cup \mathcal{D}_{\kappa}^{\star} \setminus \overline{\Gamma_{\kappa}})^{3}. \tag{A2}$$

In light of the Korn inequality [61], observe that $A(v^{\kappa}, v')$ is coercive. Moreover, the antilinear form $B(v^{\kappa}, v')$ is compact by the application of Cauchy–Schwarz inequality to $|B(v^{\kappa}, v')|$, the

compact embedding of $H^1(\mathcal{B}_\kappa^- \cup \mathcal{D}_\kappa^\star \setminus \overline{\varGamma_\kappa})^3$ into $L^2(\mathcal{B}_\kappa^- \cup \mathcal{D}_\kappa^\star \setminus \overline{\varGamma_\kappa})^3$, and the compactness of the trace operator $v^\kappa \to \llbracket v^\kappa \rrbracket$ as a map from $H^1(\mathcal{B}_\kappa^- \cup \mathcal{D}_\kappa^\star \setminus \overline{\varGamma_\kappa})^3$ to $L^2(\varGamma_\kappa)^3$ owing to the compact embedding of $\tilde{H}^{1/2}(\varGamma_\kappa)^3$ into $L^2(\varGamma_\kappa)^3$. As a result, (2.5) is of Fredholm type, and thus, is well-posed as soon as the uniqueness of a solution is guaranteed. Let $(u^f|_{\mathcal{D}_\kappa^\star \setminus \overline{\varGamma_\kappa}}, \nabla u^f|_{\mathcal{D}_\kappa^\star \setminus \overline{\varGamma_\kappa}}, t[u^f]|_{\mathcal{T}_\kappa}, t[u^f]|_{\partial \mathcal{D}_\kappa^0}) = \mathbf{0}$, then on setting $v' = v^\kappa$, observe from (A 1) that

$$\Im\left(\int_{\mathcal{D}_{\kappa}^{\star}\setminus\overline{\Gamma_{\kappa}}}\nabla\bar{\boldsymbol{v}}^{\kappa}:\boldsymbol{C}_{\kappa}:\nabla\boldsymbol{v}^{\kappa}\,\mathrm{d}V_{\xi}+\int_{\Gamma_{\kappa}}[\![\bar{\boldsymbol{v}}^{\kappa}]\!]\cdot\boldsymbol{K}_{\kappa}[\![\boldsymbol{v}^{\kappa}]\!]\,\mathrm{d}S_{\xi}\right)=0,$$

implying that $[\![v^\kappa]\!] = 0$ on Γ_κ , and $v^\kappa = 0$ in $\mathcal{D}_\kappa^\star \setminus \overline{\Gamma_\kappa}$ owing to assumption 2.2 and the first of (2.5). Note that the jump in v^κ vanishes not only on the intersection $\Gamma_\kappa \cap \partial \mathcal{D}_\kappa^\star$, but also on the perfectly continuous interface $\partial \mathcal{D}_\kappa^\star \setminus \overline{\Gamma_\kappa}$ according to the fourth of (2.5). Thus, Holmgren's theorem implies that the scattered field v^κ vanishes in an open neighbourhood of $\partial \mathcal{D}_\kappa^\star$ which by virtue of the unique continuation theorem leads to $v^\kappa(\xi) = 0$ in $\xi \in \mathcal{B} \setminus \overline{\mathcal{D}_\kappa^0}$. This completes the proof for the uniqueness of a scattering solution in $\mathcal{B}_\kappa^- \cup \mathcal{D}_\kappa^\star \setminus \overline{\Gamma_\kappa}$, and thus, substantiates the well-posedness of the forward problem.

Appendix B. Proof of lemma 4.10

Let $\hat{\mathbf{v}}$ (resp. \mathbf{v}') satisfy (2.5) for

$$X = (\hat{\mathbf{u}}|_{\mathcal{D}_{\kappa}^{\star} \setminus \overline{\Gamma_{\kappa}}}, \nabla \hat{\mathbf{u}}|_{\mathcal{D}_{\kappa}^{\star} \setminus \overline{\Gamma_{\kappa}}}, t[\hat{\mathbf{u}}]|_{\Gamma_{\kappa} \cap \overline{\mathcal{D}_{\kappa}^{\star}}} \oplus \psi, \phi), \ (\psi, \phi) \in H^{-1/2}(\Gamma_{\kappa} \setminus \overline{\mathcal{D}_{\kappa}^{\star}})^{3}) \times H^{-1/2}(\partial \mathcal{D}_{\kappa}^{0})^{3},$$
(resp.

$$X' = (\mathbf{u}'|_{\mathcal{D}_{\kappa}^{\bullet} \setminus \overline{\varGamma_{\kappa}}}, \nabla \mathbf{u}'|_{\mathcal{D}_{\kappa}^{\bullet} \setminus \overline{\varGamma_{\kappa}}}, t[\mathbf{u}']|_{\varGamma_{\kappa} \cap \overline{\mathcal{D}_{\kappa}^{\bullet}}} \oplus \psi', \phi'), \ (\psi', \phi') \in H^{-1/2}(\varGamma_{\kappa} \setminus \overline{\mathcal{D}_{\kappa}^{\bullet}})^{3}) \times H^{-1/2}(\partial \mathcal{D}_{\kappa}^{o})^{3}),$$

wherein $\nabla \cdot \mathbf{C} : \nabla \hat{\mathbf{u}} + \rho \, \omega^2 \hat{\mathbf{u}} = \mathbf{0}$ (resp. $\nabla \cdot \mathbf{C} : \nabla \mathbf{u}' + \rho \, \omega^2 \mathbf{u}' = \mathbf{0}$) in $\mathcal{D}_{\kappa'}^{\star}$, then

$$\langle T_{\kappa} \boldsymbol{X}, \boldsymbol{X}' \rangle = -\int_{\mathcal{D}_{\kappa}^{*} \setminus \overline{\Gamma_{\kappa}}} \left[\nabla \bar{\mathbf{u}}' : (\boldsymbol{C}_{\kappa} - \boldsymbol{C}) : \nabla (\hat{\mathbf{u}} + \hat{\mathbf{v}}) + \omega^{2} (\rho - \rho_{\kappa}) \bar{\mathbf{u}}' \cdot (\hat{\mathbf{u}} + \hat{\mathbf{v}}) \right] dV$$

$$+ \int_{\Gamma_{\kappa} \cap \overline{\mathcal{D}_{\kappa}^{*}}} \bar{\boldsymbol{t}} [\mathbf{u}'] \cdot [[\hat{\mathbf{v}}]] dS + \int_{\Gamma_{\kappa} \setminus \overline{\mathcal{D}_{\kappa}^{*}}} \bar{\boldsymbol{\psi}}' \cdot [[\hat{\mathbf{v}}]] dS + \int_{\partial \mathcal{D}_{\kappa}^{0}} \bar{\boldsymbol{\phi}}' \cdot (\hat{\mathbf{u}}_{\phi} + \hat{\mathbf{v}}) dS, \tag{B1}$$

where $\hat{\mathbf{u}}_{\phi}$ satisfies (4.15) with $\phi^n = \phi$. In addition, the variational form (A 1) with $\mathbf{v}^{\kappa} = \hat{\mathbf{v}}$ and $\mathbf{v}' = \mathbf{v}'$ reads

$$\int_{\mathcal{D}_{\kappa}^{*}\backslash\overline{I_{\kappa}}} \left[\nabla\bar{\mathbf{v}}': (C_{\kappa} - C): \nabla(\hat{\mathbf{u}} + \hat{\mathbf{v}}) + \omega^{2}(\rho - \rho_{\kappa})\bar{\mathbf{v}}' \cdot (\hat{\mathbf{u}} + \hat{\mathbf{v}})\right] dV
- \int_{\Gamma_{\kappa}\cap\overline{\mathcal{D}_{\kappa}^{*}}} t[\hat{\mathbf{u}}] \cdot [\![\bar{\mathbf{v}}']\!] dS - \int_{\Gamma_{\kappa}\backslash\overline{\mathcal{D}_{\kappa}^{*}}} \psi \cdot [\![\bar{\mathbf{v}}']\!] dS - \int_{\partial\mathcal{D}_{\kappa}^{0}} \phi \cdot \bar{\mathbf{v}}' dS =
- \int_{\mathcal{B}_{\kappa}^{-}\cup\mathcal{D}_{\kappa}^{*}\backslash\overline{I_{\kappa}}} \left[\nabla\bar{\mathbf{v}}': C: \nabla\hat{\mathbf{v}} - \rho\omega^{2}\bar{\mathbf{v}}' \cdot \hat{\mathbf{v}}\right] dV - \int_{\Gamma_{\kappa}} [\![\bar{\mathbf{v}}']\!] \cdot K_{\kappa} [\![\hat{\mathbf{v}}]\!] dS.$$
(B2)

Subtracting (B1) from (B2), one finds

$$-\langle T_{\kappa}X, X' \rangle = \int_{\mathcal{D}_{\kappa}^{*} \setminus \overline{\Gamma_{\kappa}}} \nabla(\bar{\mathbf{u}}' + \bar{\mathbf{v}}') : (C_{\kappa} - C) : \nabla(\hat{\mathbf{u}} + \hat{\mathbf{v}}) \, dV + \int_{\mathcal{B}_{\kappa}^{-} \cup \mathcal{D}_{\kappa}^{*} \setminus \overline{\Gamma_{\kappa}}} \nabla \bar{\mathbf{v}}' : C : \nabla \hat{\mathbf{v}} \, dV$$

$$- \int_{\Gamma_{\kappa} \cap \overline{\mathcal{D}_{\kappa}^{*}}} \left[t[\hat{\mathbf{u}}] \cdot [\![\bar{\mathbf{v}}']\!] + \bar{t}[\mathbf{u}'] \cdot [\![\hat{\mathbf{v}}]\!] \right] dS - \int_{\Gamma_{\kappa} \setminus \overline{\mathcal{D}_{\kappa}^{*}}} \left[\psi \cdot [\![\bar{\mathbf{v}}']\!] + \bar{\psi}' \cdot [\![\hat{\mathbf{v}}]\!] \right] dS$$

$$- \int_{\partial \mathcal{D}_{\kappa}^{0}} \left[\phi \cdot \bar{\mathbf{v}}' + \bar{\phi}' \cdot \hat{\mathbf{v}} + \bar{\phi}' \cdot \hat{\mathbf{u}}_{\phi} \right] dS + \int_{\Gamma_{\kappa}} [\![\bar{\mathbf{v}}']\!] \cdot K_{\kappa} [\![\hat{\mathbf{v}}]\!] dS$$

$$+ \int_{\mathcal{D}_{\kappa}^{*} \setminus \overline{\Gamma_{\kappa}}} \omega^{2} (\rho - \rho_{\kappa}) (\bar{\mathbf{u}}' + \bar{\mathbf{v}}') \cdot (\hat{\mathbf{u}} + \hat{\mathbf{v}}) dV - \int_{\mathcal{B}_{\kappa}^{-} \cup \mathcal{D}_{\kappa}^{*} \setminus \overline{\Gamma_{\kappa}}} \rho \omega^{2} \bar{\mathbf{v}}' \cdot \hat{\mathbf{v}} \, dV. \tag{B3}$$

On the other hand, adding (B1) to (B2), the result can be recast as

$$\langle T_{\kappa} X, X' \rangle = \int_{\mathcal{D}_{\kappa}^{*} \setminus \overline{\Gamma_{\kappa}}} \nabla \bar{\mathbf{u}}' : (C - C_{\kappa}) : \nabla \hat{\mathbf{u}} \, dV + \int_{\mathcal{D}_{\kappa}^{*} \setminus \overline{\Gamma_{\kappa}}} \nabla \bar{\mathbf{v}}' : C_{\kappa} : \nabla \hat{\mathbf{v}} \, dV \\
+ \int_{\mathcal{D}_{\kappa}^{*} \setminus \overline{\Gamma_{\kappa}}} \left[\nabla \bar{\mathbf{u}}' : (C - C_{\kappa}) : \nabla \hat{\mathbf{v}} \, dV - \nabla \bar{\mathbf{v}}' : (C - C_{\kappa}) : \nabla \hat{\mathbf{u}} \right] dV + \int_{\mathcal{B}_{\kappa}^{-}} \nabla \bar{\mathbf{v}}' : C : \nabla \hat{\mathbf{v}} \, dV \\
+ \int_{\Gamma_{\kappa} \cap \overline{\mathcal{D}_{\kappa}^{*}}} \left[\bar{t} [\mathbf{u}'] \cdot [[\hat{\mathbf{v}}]] - t [\hat{\mathbf{u}}] \cdot [[\bar{\mathbf{v}}']] \right] dS + \int_{\Gamma_{\kappa} \setminus \overline{\mathcal{D}_{\kappa}^{*}}} \left[\bar{\psi}' \cdot [[\hat{\mathbf{v}}]] - \psi \cdot [[\bar{\mathbf{v}}']] \right] dS \\
+ \int_{\partial \mathcal{D}_{\kappa}^{0}} \left[\bar{\phi}' \cdot (\hat{\mathbf{u}}_{\phi} + \hat{\mathbf{v}}) - \phi \cdot \bar{\mathbf{v}}' \right] dS + \int_{\Gamma_{\kappa}} [[\bar{\mathbf{v}}']] \cdot K_{\kappa} [[\hat{\mathbf{v}}]] dS \\
- \int_{\mathcal{D}_{\kappa}^{*} \setminus \overline{\Gamma_{\kappa}}} \omega^{2} (\rho - \rho_{\kappa}) (\bar{\mathbf{u}}' - \bar{\mathbf{v}}') \cdot (\hat{\mathbf{u}} + \hat{\mathbf{v}}) dV - \int_{\mathcal{B}_{\kappa}^{-} \cup \mathcal{D}_{\kappa}^{*} \setminus \overline{\Gamma_{\kappa}}} \rho \omega^{2} \bar{\mathbf{v}}' \cdot \hat{\mathbf{v}} \, dV. \tag{B4}$$

In light of (B3) and (B4), define $T_{\circ}^{\pm}:\mathfrak{S}(H_{\Delta})\to \tilde{S}(\mathcal{D}_{\kappa}^{\star}\cup \Gamma_{\kappa}\cup\partial\mathcal{D}_{\kappa}^{0})$ such that

$$\begin{cases}
-\langle T_{\circ}^{-}X, X' \rangle = \int_{\mathcal{D}_{\kappa}^{*} \setminus \overline{\Gamma_{\kappa}}} \nabla(\bar{\mathbf{u}}' + \bar{\mathbf{v}}') : (C_{\kappa} - C) : \nabla(\hat{\mathbf{u}} + \hat{\mathbf{v}}) \, dV \\
+ \int_{\mathcal{B}_{\kappa}^{-} \cup \mathcal{D}_{\kappa}^{*} \setminus \overline{\Gamma_{\kappa}}} \nabla \bar{\mathbf{v}}' : C : \nabla \hat{\mathbf{v}} \, dV + \int_{\mathcal{D}_{\kappa}^{*} \setminus \overline{\Gamma_{\kappa}}} \bar{\mathbf{u}}' \cdot \hat{\mathbf{u}} \, dV, \\
\langle T_{\circ}^{+}X, X' \rangle = \int_{\mathcal{D}_{\kappa}^{*} \setminus \overline{\Gamma_{\kappa}}} \nabla \bar{\mathbf{u}}' : (C - C_{\kappa}) : \nabla \hat{\mathbf{u}} \, dV + \int_{\mathcal{D}_{\kappa}^{*} \setminus \overline{\Gamma_{\kappa}}} \nabla \bar{\mathbf{v}}' : C_{\kappa} : \nabla \hat{\mathbf{v}} \, dV \\
+ \int_{\mathcal{D}_{\kappa}^{*} \setminus \overline{\Gamma_{\kappa}}} \left[\nabla \bar{\mathbf{u}}' : (C - C_{\kappa}) : \nabla \hat{\mathbf{v}} \, dV - \nabla \bar{\mathbf{v}}' : (C - C_{\kappa}) : \nabla \hat{\mathbf{u}} \right] dV \\
+ \int_{\mathcal{B}^{-}} \nabla \bar{\mathbf{v}}' : C : \nabla \hat{\mathbf{v}} \, dV + \int_{\mathcal{D}^{*} \setminus \overline{\Gamma_{\kappa}}} \bar{\mathbf{u}}' \cdot \hat{\mathbf{u}} \, dV.
\end{cases} \tag{B5}$$

Given assumption 4.5, it is evident that $\Re(e^{i\theta}T_{\circ}^{-})$ is coercive on $\mathfrak{S}(H_{\Delta})$ for $\theta=[0\,\pi/2)$ provided that the first of assumption 4.8 holds. In the second case of the latter, however, one may show that $\Re(T_{\circ}^{+})$ is coercive on $\mathfrak{S}(H_{\Delta})$ by following the argument used in the proof of ([32], theorem 2.47). Now, by deploying the Rellich compact embeddings along with the regularity of the trace operator, one concludes that

$$T_{\rm c} := \Re(T_{\kappa} - T_{\circ}^{\pm}) : \mathfrak{S}(H_{\Delta}) \to \tilde{S}(\mathcal{D}_{\kappa}^{\star} \cup \Gamma_{\kappa} \cup \partial \mathcal{D}_{\kappa}^{0})$$

is compact.

References

- 1. Pokharel R, Brown DW, Clausen B, Byler DD, Ickes TL, McClellan KJ, Suter RM, Kenesei P. 2017 Non-destructive characterization of UO_{2+x} nuclear fuels. *Microscopy Today* **25**, 42–47. (doi:10.1017/S155192951700102X)
- Bond LJ. 2015 Needs and opportunities: nondestructive evaluation for energy systems. In Smart materials and nondestructive evaluation for energy systems 2015, vol. 9439, p. 943902. International Society for Optics and Photonics.
- 3. Balitskii OI, Kvasnytska YH, Ivaskevych LM, Mialnitsa HP, Kvasnytska KH. 2022 Fatigue fracture of the blades of gas-turbine engines made of a new refractory nickel alloy. *Mater. Sci.* 57, 475–483. (doi:10.1007/s11003-022-00568-z)
- 4. Arregui-Mena JD *et al.* 2022 Qualitative and quantitative analysis of neutron irradiation effects in SiC/SiC composites using X-ray computed tomography. *Compos. Part B: Eng.* **238**, 109896. (doi:10.1016/j.compositesb.2022.109896)
- 5. Terrani K. 2018 Accident tolerant fuel cladding development: Promise, status, and challenges. *J. Nucl. Mater.* **501**, 13–30. (doi:10.1016/j.jnucmat.2017.12.043)
- Nucl. Mater. 501, 13–30. (doi:10.1016/j.jnucmat.2017.12.043)
 del Río JS, Pascual-Gonzalez C, Martinez V, Jiménez JL, Gonzalez C. 2021 3D-printed resistive carbon-fiber-reinforced sensors for monitoring the resin frontal flow during composite

manufacturing. Sens. Actuators, A 317, 112422.

- 7. Van der Heijden A. 2018 Developments and challenges in the manufacturing, characterization and scale-up of energetic nanomaterials—a review. *Chem. Eng. J.* **350**, 939–948. (doi:10.1016/j.cej.2018.06.051)
- 8. Meier C, Weissbach R, Weinberg J, Wall WA, Hart AJ. 2019 Critical influences of particle size and adhesion on the powder layer uniformity in metal additive manufacturing. *J. Mater. Process. Technol.* **266**, 484–501. (doi:10.1016/j.jmatprotec.2018.10.037)
- 9. Netzelmann U, Mross A, Waschkies T, Weber D, Toma E, Neurohr H. 2022 Nondestructive testing of the integrity of solid oxide fuel cell stack elements by ultrasound and thermographic techniques. *Energies* **15**, 831. (doi:10.3390/en15030831)
- 10. Yan G, Raetz S, Chigarev N, Gusev VE, Tournat V. 2018 Characterization of progressive fatigue damage in solid plates by laser ultrasonic monitoring of zero-group-velocity lamb modes. *Phys. Rev. Appl.* **9**, 061001. (doi:10.1103/PhysRevApplied.9.061001)
- 11. Beaumont PWR. 2017 Slow cracking in composite materials: catastrophic fracture of composite structures. In *The structural integrity of carbon fiber composites*, pp. 489–528. New York, NY: Springer.
- 12. Roy S, Kumar A, Li S. 2017 A nano-micro-macro-multiscale model for progressive failure prediction in advanced composites. In *The structural integrity of carbon fiber composites*, pp. 137–169. New York, NY: Springer.
- 13. Amin MG. 2017 Through-the-wall radar imaging. New York, NY: CRC press.

Downloaded from https://royalsocietypublishing.org/ on 04 June 2023

- 14. Faria JJ, Fonseca LG, de Faria AR, Cantisano A, Cunha TN, Jahed H, Montesano J. 2022 Determination of the fatigue behavior of mechanical components through infrared thermography. *Eng. Fail. Anal.* **134**, 106018. (doi:10.1016/j.engfailanal.2021.106018)
- 15. Zhao Q, Dan X, Sun F, Wang Y, Wu S, Yang L. 2018 Digital shearography for NDT: phase measurement technique and recent developments. *Appl. Sci.* **8**, 2662. (doi:10.3390/app8122662)
- 16. Garcea S, Wang Y, Withers P. 2018 X-ray computed tomography of polymer composites. *Compos. Sci. Technol.* **156**, 305–319. (doi:10.1016/j.compscitech.2017.10.023)
- 17. Bychkov A, Simonova V, Zarubin V, Cherepetskaya E, Karabutov A. 2018 The progress in photoacoustic and laser ultrasonic tomographic imaging for biomedicine and industry: a review. *Appl. Sci.* **8**, 1931. (doi:10.3390/app8101931)
- 18. Zhang J, Niu X, Croxford AJ, Drinkwater BW. 2022 Strategies for guided acoustic wave inspection using mobile robots. *Proc. R. Soc. A* 478, 20210762. (doi:10.1098/rspa.2021.0762)
- Bakre C, Afzalimir SH, Jamieson C, Nassar A, Reutzel EW, Lissenden CJ. 2022 Laser generated broadband rayleigh waveform evolution for metal additive manufacturing process monitoring. *Appl. Sci.* 12, 12208. (doi:10.3390/app122312208)
- 20. Zhang J, Wu J, Zhao X, Yuan S, Ma G, Li J, Dai T, Chen H, Yang B, Ding H. 2020 Laser ultrasonic imaging for defect detection on metal additive manufacturing components with rough surfaces. *Appl. Opt.* **59**, 10380–10388. (doi:10.1364/AO.405284)
- Wilcox PD, Croxford AJ, Budyn N, Bevan RL, Zhang J, Kashubin A, Cawley P. 2020 Fusion of multi-view ultrasonic data for increased detection performance in non-destructive evaluation. *Proc. R. Soc. A* 476, 20200086. (doi:10.1098/rspa.2020.0086)
- 22. Zhang X, Fincke JR, Wynn CM, Johnson MR, Haupt RW, Anthony BW. 2019 Full noncontact laser ultrasound: first human data. *Light: Sci. Appl.* 8, 1–11.
- 23. Davies SJ, Edwards C, Taylor GS, Palmer SB. 1993 Laser-generated ultrasound: its properties, mechanisms and multifarious applications. *J. Phys. D: Appl. Phys.* **26**, 329. (doi:10.1088/0022-3727/26/3/001)
- 24. Zimermann R *et al.* 2021 Multi-layer ultrasonic imaging of as-built wire+ Arc Additive manufactured components. *Addit. Manuf.* 48, 102398.
- 25. Liu S *et al.* 2022 Inspection of the internal defects with different size in Ni and Ti additive manufactured components using laser ultrasonic technology. *Opt. Laser Technol.* **146**, 107543. (doi:10.1016/j.optlastec.2021.107543)
- 26. Chen Y, Lu L, Karniadakis GE, Dal Negro L. 2020 Physics-informed neural networks for inverse problems in nano-optics and metamaterials. *Opt. Express* **28**, 11618–11633. (doi:10.1364/OE.384875)
- 27. Chen Y, Dal Negro L. 2022 Physics-informed neural networks for imaging and parameter retrieval of photonic nanostructures from near-field data. *APL Photonics* 7, 010802. (doi:10.1063/5.0072969)
- 28. Van Sloun RJ, Cohen R, Eldar YC. 2019 Deep learning in ultrasound imaging. *Proc. IEEE* **108**, 11–29. (doi:10.1109/JPROC.2019.2932116)

- 29. Cantero-Chinchilla S, Wilcox PD, Croxford AJ. 2022 Deep learning in automated ultrasonic NDE–developments, axioms and opportunities. *NDT & E Int.* **131**, 102703.
- 30. Arinez JF, Chang Q, Gao RX, Xu C, Zhang J. 2020 Artificial intelligence in advanced manufacturing: current status and future outlook. *J. Manuf. Sci. Eng.* **142**, 110804. (doi:10.1115/1.4047855)
- 31. Cakoni F, Colton D, Haddar H. 2020 A duality between scattering poles and transmission eigenvalues in scattering theory. *Proc. R. Soc. A* **476**, 20200612. (doi:10.1098/rspa.2020.0612)
- 32. Cakoni F, Colton D, Haddar H. 2016 *Inverse scattering theory and transmission eigenvalues*. Society for Industrial and Applied Mathematics.
- 33. Audibert L, Haddar H. 2017 The generalized linear sampling method for limited aperture measurements. *SIAM J. Imag. Sci.* **10**, 845–870. (doi:10.1137/16M110112X)
- 34. Guzina BB, Pourahmadian F. 2015 Why the high-frequency inverse scattering by topological sensitivity may work. *Proc. R. Soc. A* **471**, 20150187. (doi:10.1098/rspa.2015.0187)
- 35. Bonnet M, Cakoni F. 2019 Analysis of topological derivative as a tool for qualitative identification. *Inverse Prob.* 35, 104007. (doi:10.1088/1361-6420/ab0b67)
- Narumanchi VV, Pourahmadian F, Lum J, Townsend A, Tringe JW, Stobbe DM, Murray TW.
 2022 Laser ultrasonic imaging of subsurface defects with the linear sampling method. Opt. Express
- 37. Audibert L, Girard A, Haddar H. 2015 Identifying defects in an unknown background using differential measurements. *Inverse Probl. Imag.* **9**, 625–643. (doi:10.3934/ipi.2015.9.625)
- 38. Nguyen TP. 2020 Differential imaging of local perturbations in anisotropic periodic media. *Inverse Prob.* **36**, 034004. (doi:10.1088/1361-6420/ab2066)
- Audibert L, Chesnel L, Haddar H, Napal K. 2021 Qualitative indicator functions for imaging crack networks using acoustic waves. SIAM J. Sci. Comput. 43, B271–B297. (doi:10.1137/20M134650X)
- Pourahmadian F, Haddar H. 2020 Differential tomography of micromechanical evolution in elastic materials of unknown micro/macrostructure. SIAM J. Imag. Sci. 13, 1302–1330. (doi:10.1137/19M1305707)
- 41. Pourahmadian F. 2021 Experimental validation of differential evolution indicators for ultrasonic imaging in unknown backgrounds. *Mech. Syst. Signal Process.* **161**, 108029. (doi:10.1016/j.ymssp.2021.108029)

Downloaded from https://royalsocietypublishing.org/ on 04 June 2023

- 42. Charalambopoulos A. 2002 On the interior transmission problem in nondissipative, inhomogeneous, anisotropic elasticity. *J. Elast. Phys. Sci. Solids* **67**, 149–170.
- 43. Charalambopoulos A, Gintides D, Kiriaki K. 2002 The linear sampling method for the transmission problem in three-dimensional linear elasticity. *Inverse Prob.* **18**, 547. (doi:10.1088/0266-5611/18/3/303)
- 44. Charalambopoulos A, Anagnostopoulos KA. 2008 On the spectrum of the interior transmission problem in isotropic elasticity. *J. Elast.* **90**, 295–313. (doi:10.1007/s10659-007-9146-9)
- 45. Charalambopoulos A, Kirsch A, Anagnostopoulos KA, Gintides D, Kiriaki K. 2006 The factorization method in inverse elastic scattering from penetrable bodies. *Inverse Prob.* **23**, 27. (doi:10.1088/0266-5611/23/1/002)
- 46. Bellis C, Guzina BB. 2010 On the existence and uniqueness of a solution to the interior transmission problem for piecewise-homogeneous solids. *J. Elast.* **101**, 29–57. (doi:10.1007/s10659-010-9242-0)
- 47. Bellis C, Cakoni F, Guzina BB. 2013 Nature of the transmission eigenvalue spectrum for elastic bodies. *IMA J. Appl. Math.* **78**, 895–923. (doi:10.1093/imamat/hxr070)
- 48. Cakoni F, Kow PZ, Wang JN. 2021 The interior transmission eigenvalue problem for elastic waves in media with obstacles. *Inverse Probl. Imag.* **15**, 445. (doi:10.3934/ipi.2020075)
- 49. Lach TG, Silva CM, Zhou Y, Boldman WL, Rack PD, Weber WJ, Zhang Y. 2022 Dynamic substrate reactions during room temperature heavy ion irradiation of CoCrCuFeNi high entropy alloy thin films. *npj Mater. Degradat.* **6**, 1–15.
- 50. Lieou CKC, Bronkhorst CA. 2021 Thermomechanical conversion in metals: dislocation plasticity model evaluation of the Taylor-Quinney coefficient. *Acta Mater.* **202**, 170–180. (doi:10.1016/j.actamat.2020.10.037)
- 51. Barenblatt GI. 2003 Scaling (Cambridge texts in applied mathematics). Cambridge, UK: Cambridge University Press.
- 52. Lo KK. 1978 Analysis of branched cracks. J. Appl. Mech. 45, 797-802. (doi:10.1115/1.3424421)

- 53. Daux C, Moës N, Dolbow J, Sukumar N, Belytschko T. 2000 Arbitrary branched and intersecting cracks with the extended finite element method. *Int. J. Numer. Methods Eng.* 48, 1741–1760. (doi:10.1002/1097-0207(20000830)48:12<1741::AID-NME956>3.0.CO;2-L)
- 54. Mukai DJ, Ballarini R, Miller GR. 1990 Analysis of branched interface cracks. *J. Appl. Mech.* 57, 887–893. (doi:10.1115/1.2897657)
- 55. Goswami S, Becker W. 2012 Computation of 3-D stress singularities for multiple cracks and crack intersections by the scaled boundary finite element method. *Int. J. Fract.* **175**, 13–25. (doi:10.1007/s10704-012-9694-2)
- 56. Mendelsohn DA. 1984 A review of hydraulic fracture modeling II: 3D modeling and vertical growth in layered rock. *J. Energy Res. Technol.* **106**, 543–553. (doi:10.1115/1.3231121)
- 57. Atkinson C. 1977 On stress singularities and interfaces in linear elastic fracture mechanics. *Int. J. Fract.* **13**, 807–820. (doi:10.1007/BF00034324)
- 58. Hähner P. 2000 On the uniqueness of the shape of a penetrable, anisotropic obstacle. *J. Comput. Appl. Math.* **116**, 167–180.
- 59. Kirsch A, Grinberg N. 2008 *The factorization method for inverse problems*, **vol. 36**. Oxford, UK: Oxford University Press.
- 60. Bonnet M. 1999 Boundary integral equations methods for solids and fluids. Hoboken, NJ: Wiley.
- 61. Pourahmadian F, Guzina BB, Haddar H. 2017 Generalized linear sampling method for elastic-wave sensing of heterogeneous fractures. *Inverse Prob.* **33**, 055007. (doi:10.1088/1361-6420/33/5/055007)